Integrated optimization model for hydrogen supply chain network design and hydrogen fueling station planning

Lei Li, Hervé Manier, Marie-Ange Manier

Version of Record: https://www.sciencedirect.com/science/article/pii/S0098135419305757
Manuscript_9c22c3c230e9a69131c9bfe54d879164

Integrated optimization model for hydrogen supply chain network design and hydrogen fueling station planning

Lei Li[a,*], Hervé Manier[a], Marie-Ange Manier[a]

[a] *Univ. Bourgogne Franche-Comté FEMTO-ST Institute/CN RS, UTBM, rue Thierry-Mieg, 90 010 Belfort Cedex, France*

Abstract

This paper focuses on developing a mathematical model that covers the entire hydrogen supply network. The classical hydrogen supply chain network design (HSCND) model is integrated with the hydrogen fueling station planning (HFSP) model to generate a new formulation. The proposed model considers the feedstock supply, the installation and operation of hydrogen facilities, the operation of transportation technologies, and the carbon capture and storage (CCS) system. Two primary hydrogen fueling technologies, namely on-site fueling (hydrogen is produced on-site) and standard fueling (hydrogen is delivered by road), are considered. The problem is formulated as a mixed-integer linear programming (MILP) model that minimizes the least cost of hydrogen (LCOH). The necessity of considering various components within a single framework is demonstrated through a case study in Franche-Comté, France. The role of each key model component (such as the fueling technology, feedstock transportation, and CCS system) is analyzed. The proposed model is capable of studying the interactions that exist between different parts of a hydrogen supply network. Consequently, more comprehensive construction plans for the HSCN are guaranteed.

Keywords: Integration, Optimization model, Hydrogen supply chain network, Hydrogen fueling station, MILP.

1. Introduction

The transportation sector is one of the most significant contributors to greenhouse gas (GHG) emissions. It accounted for 26% of EU, 28% of U.S., and 23% worldwide of total GHG emissions in

Abbreviations: BG, biomass gasification; CCS, carbon capture and storage; FCEV, fuel cell electric vehicle; FCLM, flow-capturing location model; GH_2, gaseous hydrogen; HFSP, hydrogen fueling station planning; HSCN, hydrogen supply chain network; HSCND, hydrogen supply chain network design; LCOH, least cost of hydrogen; LH_2, liquid hydrogen; MILP, mixed-integer linear programming; OD, origin–destination; SMR, steam methane reforming;

*Corresponding author

Email addresses: lei.li1@utbm.fr; lilei.utbm@gmail.com (Lei Li), herve.manier@utbm.fr (Hervé Manier), marie-ange.manier@utbm.fr (Marie-Ange Manier)

recent years (Environmental Protection Agency, 2018; European Environment Agency, 2017; Sims et al., 2014). Within the sector, road transportation is by far the largest category, contributing approximately three-quarters of all emissions (International Energy Agency, 2015). Aggressive and sustained mitigation strategies are essential if deep GHG reduction ambitions, such as the two-degree scenario, are to be achieved. To this end, the equivalent of 160 million low-emission vehicles will need to be on the roads by 2030, according to International Energy Agency (2017).

It is widely accepted that hydrogen is a critical element in the decarbonization of the transportation sector, which still relies almost exclusively on oil (McKinsey & Company, 2017). Hydrogen can be used in electric vehicles (EVs) equipped with hydrogen fuel cells (FCEV). FCEVs are a necessary complement to battery electric vehicles (BEVs) as FCEVs add convenience for consumers with long ranges and fast fueling times. FCEVs can also provide potentially very low carbon emissions (International Energy Agency, 2015). In terms of cost per mile, FCEVs will need tax credits or other subsidies to be competitive with conventional cars and other types of alternative fuel vehicles during the early stages of commercial implementation (M. Ruth, T.A. Timbario & Laffen, 2011). However, significant cost reduction can be realized by scaling up manufacturing of FCEVs and hydrogen fueling infrastructures (McKinsey & Company, 2017).

Although the potential environmental benefits of hydrogen in the transportation sector are promising, the shift towards a hydrogen economy is challenging. Currently, the sales of FCEVs look bleak. In the U.S., only about 1,800 Mirai (a mid-size FCEV manufactured by Toyota) have been shipped in 2017. In contrast, 60 times as many Priuses (a hybrid electric vehicle) have been sold, and Tesla has also delivered more than 50,000 electric vehicles (Carsalesbase, 2018). The sluggish pace of sales for FCEVs is in part explained by the fact that only 65 hydrogen fueling stations were available in 2017, compared to more than 20,000 charging stations across the U.S. (Department of Energy, 2018a). This situation is often described as a "chicken-and-egg" problem (Achtnicht et al., 2012). Investments in fueling infrastructures pay off only if the vehicle number grows, but developing, building, and marketing vehicles are viable only with adequate fueling stations (McKinsey & Company, 2017).

One way to solve this dilemma is to coordinate the roll-out of vehicles and infrastructure development. Suppose that automobile manufacturers have chosen specific cities or areas as a target. Fuel providers would need to create a construction plan to realize the coordination. Such a plan involves two essential characteristics: (i) it should focus on planning the initial development of infrastructures while accounting for the full range of local factors, such as geographic distribution of feedstocks for hydrogen production and anticipated hydrogen demand at the fueling stations; (ii) it should be an integrated plan, which means that all types of infrastructures (hydrogen production plants, fueling stations, and CO_2 storage sites) are considered simultaneously. A simple example of a hydrogen supply network is illustrated in Fig. 1.

Hydrogen is produced at a plant using biomass that is transported from a biomass warehouse. The CO_2 emissions from hydrogen production are captured and transported to a CO_2 storage site.

Hydrogen is delivered to fueling stations and other types of consumers (e.g., a fleet of buses or stationary applications). There are also fueling stations that run autonomously, they produce hydrogen on-site, thus do not rely on delivery. The construction plan is responsible for answering the following questions: What is the hydrogen demand, and where is this demand located? What kind of feedstock and technology should be selected to produce hydrogen? Will hydrogen be produced on-site or be delivered from production plants? How many production plants and fueling stations are needed, and where will they be located? What are the most suitable types of transportation (either for hydrogen or for feedstock)?

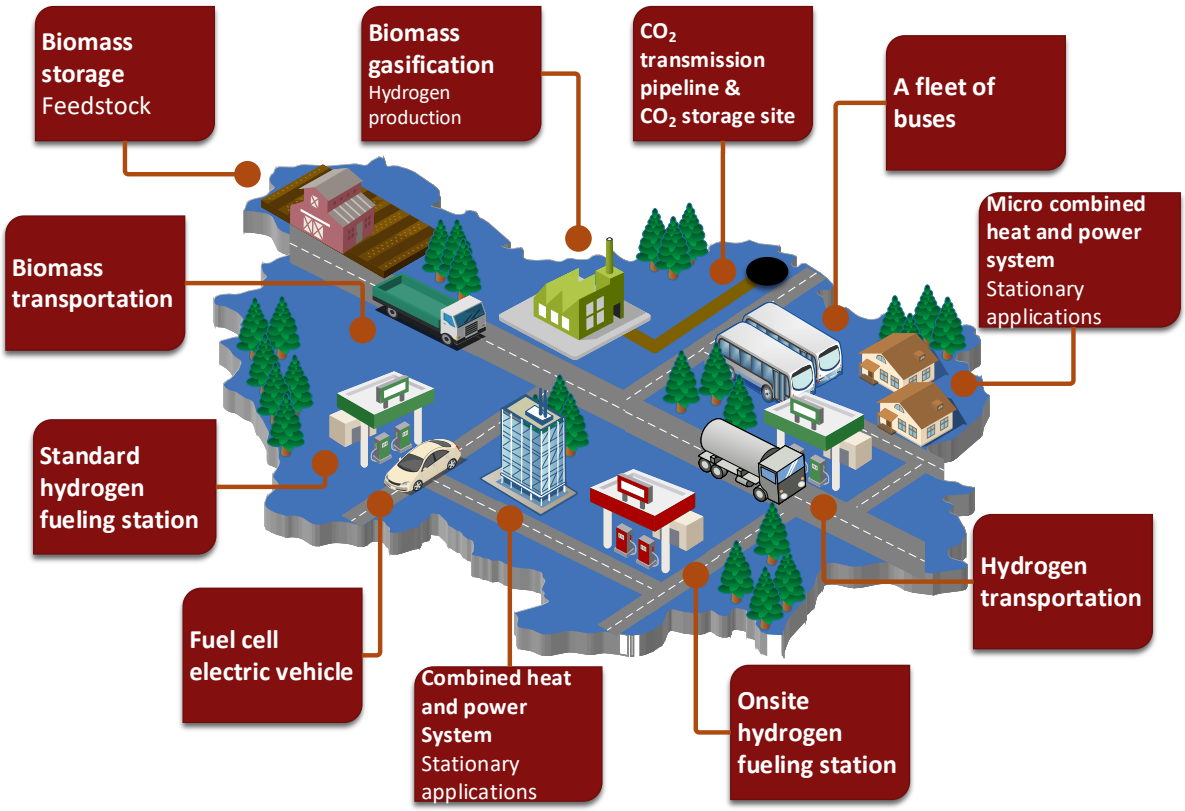

Figure 1: A simple example of hydrogen supply network

These questions are difficult to answer without using mathematical models because technological and spatial interactions exist between the different parts of the network. Several models for hydrogen networks have been developed, and they typically fall into one of the following two categories Li et al. (2019):

- Hydrogen supply chain network design (HSCND) models: these models include multiple components such as feedstock, production, storage, and transportation. They focus on long-

term planning and usually run on a national scale.

- Hydrogen fueling station planning (HFSP) models: these models determine the optimal location of hydrogen fueling stations. They focus on the initial development of infrastructures and are generally applied at a city or regional level.

Unfortunately, neither the HSCND nor the HFSP models are qualified to develop the construction plan described above. The main reason is that neither considers the entire hydrogen supply network. Most HSCND models involve no decision variables related to fueling station issues. Those that do consider fueling infrastructures determine only the number, type (gaseous or liquefied hydrogen), and size of the stations. On the other hand, the HFSP models do not answer questions like "where will the hydrogen come from?". They are less concerned with the technologies of the stations, and therefore do not include upstream infrastructure issues. Thus, it is reasonable to combine these two types to build a new model that can cover all types of infrastructures within the hydrogen supply network. In addition, the time horizon and geographic scale should be carefully selected to coordinate the characteristics of these two model classes. In light of these concerns, the main contributions of this paper are:

- Propose for the first time a mathematical model that covers the entire hydrogen supply network (from feedstock supply to fueling stations).

- Demonstrate the necessity of considering various components within a single framework.

The remainder of this paper is divided into six main sections. Section 2 analyzes the relevant scientific literature. Section 3 provides the problem description. Section 4 presents the proposed mathematical model. Section 5 describes the setup of instances as well as the input data. Section 6 presents the results and discussions. Finally, Section 7 provides the conclusions and outlines some plans for future development.

2. Literature review

Substantial work has been done in both the fields of hydrogen supply network design and fueling station planning. The relevant literature is briefly reviewed in this section.

2.1. Hydrogen supply chain network design (HSCND)

The HSCND models fall into the category of geographically explicit optimization models. Binary and integer decision variables are employed to address location of facilities, sizing decisions, selection of suitable production technologies, and selection of transportation modes between facilities. Because product flows along the supply chain are modeled by continuous constraints, these models are often mixed-integer formulations (Eskandarpour et al., 2015). According to Agnolucci

& Mcdowall (2013), three representative HSCND models have been developed by Almansoori & Shah (2006) , Parker et al. (2010), and Johnson & Ogden (2012).

Parker et al. (2010) focused on evaluating the infrastructure requirements of hydrogen production from agricultural residues. A mixed-integer nonlinear programming model based on geographic information systems (GIS) was constructed for finding the most efficient and economical configuration. Johnson & Ogden (2012) provided a network optimization tool for identifying the lowest cost centralized production and pipeline transmission infrastructure within real geographic regions. The model identifies the number, size, and location of production facilities and the diameter, length, and location of transmission pipeline corridors.

Almansoori & Shah (2006) established a steady state "snapshot" model that integrates multiple components within a single framework. They selected Great Britain as a case study. Later, Almansoori & Shah (2009) extended their study by considering the availability of feedstocks and their logistics, as well as the variation of hydrogen demand over a long-term planning horizon leading to phased infrastructure development. The objective function in the model comprises both operational and investment costs, split in terms of production, storage, transportation, and feedstocks. The work of Almansoori & Shah (2006) is the seminal paper in this branch of the literature. It has been a source of inspiration for other studies, which have attempted to improve it through multiple modifications (Li et al., 2019), such as introducing multi-objective optimization (De-León Almaraz et al., 2015; Guillén-Gosálbez et al., 2010; Kim & Moon, 2008), multi-period optimization (Moreno-Benito et al., 2017; Murthy Konda et al., 2011; Ogumerem et al., 2018), uncertainty issues (Kim et al., 2008), and integrating it with other supply chains (Agnolucci et al., 2013; Cho et al., 2016; Hwangbo et al., 2017; Won et al., 2017; Woo et al., 2016).

Melo et al. (2009) highlighted the importance of explicitly integrating the feedstock issues into SCND. However, less than half the studies cited above involve the feedstock and its logistics into modeling, as shown in Table 1. It is also noted that few papers consider the possible adoption of a CCS (carbon capture and storage) system, which is of great importance to meet specific carbon targets when fossil energy is chosen as the feedstock. Little attention has been paid to the strategic decisions related to the fueling station in HSCND models. Neither the location problem nor the technology selection (i.e., standard or on-site) has been investigated. It is noteworthy that whether an HSCN is based on liquid hydrogen (LH_2) or gaseous hydrogen (GH_2) is determined subjectively through the definition of scenarios or configurations in most models.

2.2. Hydrogen fueling station planning (HFSP)

Most papers published in this field concentrate on the location-allocation problem of fueling stations. Optimization-based approaches for locating fueling stations are divided into two main groups depending on the geometric representation of demands, which are models for node-based and flow-based demands (Hosseini & MirHassani, 2015).

Table 1: Strategic decisions in HSCND models

Articles	Feed.	Prod.	Transp.	CCS	Fueling station			
					Nb.	Lo.	Size	Tech.
Agnolucci et al. (2013)		✔	✔	✔	✔		✔	
Almansoori & Shah (2006)		✔	✔					
Almansoori & Shah (2009)	✔	✔	✔					
Cho et al. (2016)	✔	✔	✔					
Copado-Méndez et al. (2013)		✔	✔					
De-León Almaraz et al. (2015)	✔	✔	✔		✔			
Guillén-Gosálbez et al. (2010)		✔	✔					
Hwangbo et al. (2017)		✔	✔					
Johnson & Ogden (2012)		✔	✔	✔				
Kim & Moon (2008)		✔	✔					
Kim et al. (2008)		✔	✔					
Murthy Konda et al. (2011)		✔	✔	✔	✔			
Moreno-Benito et al. (2017)	✔	✔	✔	✔	✔			
Ogumerem et al. (2018)	✔	✔	✔					
Parker et al. (2010)	✔	✔	✔					
Samsatli & Samsatli (2015)	✔	✔	✔					
Van Den Heever & Grossmann (2003)		✔	✔					
Won et al. (2017)		✔	✔					
Woo et al. (2016)	✔	✔	✔		✔		✔	
This study	✔	✔	✔	✔	✔	✔	✔	✔

Feed.: Feedstock and its transportation; Prod.: Hydrogen production;
Transp.: Hydrogen transportation; CCS: Carbon capture and storage;
Nb.: Number; Lo.: Location; Tech.: Technology.

The node-based demand models consider each node as a demand point, and drivers would have to make specific trips to the facilities to obtain services. The main advantage of using these models is the relatively easy access to data, such as population and spatial information (Hwang et al., 2015). Nicholas et al. (2004) and Nicholas & Ogden (2006) employed the p-median model, which is one of the node-based demand models, to locate fueling stations that minimize a weighted sum of driving times to the closest station. Lin et al. (2008) also applied the p-median model to the fuel-travel-back concept and proposed a MILP formulation that minimizes the total fuel-travel-back time. Another example refers to the California Hydrogen Infrastructure Tool (CHIT), which is a geospatial analysis tool to identify the areas with the greatest need for fueling infrastructure based on a gap analysis between a projected market and current infrastructure (California Air Resources Board, 2018).

Many researchers argue that for fueling stations, as well as other service stations such as automatic teller machines, customer demand does not occur entirely at points, because people commonly will not make a trip solely for such a service (Jung et al., 2014). It may be more

realistic to model the demands as *flows* on the network, which are served "on the way". This consideration leads to the development of flow-based models (Huang et al., 2015). First developed by Berman et al. (1992) and Hodgson (1990), the Flow-Capturing Location Model (FCLM) is a maximum coverage model that entails facility locations to serve passing flows, which are considered as captured if a facility is located on the flow paths. The basic model locates p facilities to capture as much flow as possible. Many modifications have been made to extend the original FCLM, such as introducing budget constraints (Shukla et al., 2011), considering the limited driving range of vehicles (Kuby & Lim, 2005; Kuby et al., 2009; Lim & Kuby, 2010), relaxing the assumption that all flows are on the shortest path between Origin–Destination pairs (Berman et al., 1995; Kim & Kuby, 2012, 2013), and introducing fueling capacities (Hosseini & MirHassani, 2017; Hosseini et al., 2017; Upchurch et al., 2009). Apart from the FCLM, there is another series of flow-based models that aim to satisfy all travel demands by deploying the least number of fueling stations (Wang & Lin, 2009, 2013; Wang & Wang, 2010).

While considerable attention has been paid to the location problem of fueling stations, the influence of fueling technology on location decisions has not been given the attention it needs. It will be demonstrated in the following sections that the fueling network is deeply impacted by the selection of fueling technology (on-site or standard). It must also be noted that, for many flow-based models, the relationship between the captured flow and the fueling capacity has been neglected. In short, models cited above could tell "where" to locate the station, but neither the information on "what it is" (the fueling technology) nor "how big it is" (the size) is provided.

2.3. Literature summary

The existing literature reveals a gap in the development of comprehensive hydrogen supply network models. Some researchers have already noticed this issue. He et al. (2017) and Sun et al. (2017) have proposed hydrogen station siting optimization models, which focus on the stage of hydrogen source-hydrogen station. Their models optimize the number and locations of stations, hydrogen source selection for the stations, and method of transportation to minimize the hydrogen life cycle cost. However, the capacity of each station is pre-defined. Furthermore, the feedstock and its logistics, as well as a CCS system, have not been considered in the models. There is no decision variable relating to fueling technologies.

It is the primary purpose of this paper to fill the research gap by integrating the hydrogen supply chain network design and hydrogen fueling station planning. Also, feedstock and CCS issues are involved, and the model can decide the fueling technology and fueling capacity.

3. Problem description

The model was developed to solve the problem summarized below. Given

- The estimated total amount of hydrogen consumed by FCEVs within a region, and spatial description of the region represented by an undirected graph. Each node denotes a city or a large town and is characterized by
  - Demographic metrics (see Section 5)
  - Availability of each type of feedstock
  - Existence of a potential CO_2 storage site and its processing capacity
  - Existence of fixed-location demand and its amount
- A set of feedstocks, with each feedstock having the following properties:
  - Unit cost associated with its purchase
  - Correspondent production technology and transportation technology (if needed)
  - Number of units for producing 1 kg of hydrogen
- A set of production technologies, each is characterized by its:
  - Product form (gaseous or liquid hydrogen)
  - Capital, operating costs, and production capacity
  - Upstream emission factor, relating to the emissions produced by the feedstock consumed and other energy inputs during their upstream processing (i.e., extraction, production, and transportation)
  - On-site emission factor, relating to the emissions from the production procedure
  - Emission capture efficiency, the percent of on-site emissions that can be captured if a CCS system is employed
- A set of fueling technologies (standard and on-site), each is characterized by
  - The form of hydrogen it receives (standard fueling)
  - Correspondent type of feedstock (on-site fueling)
  - Feedstock demand (on-site fueling)
  - Minimum and maximum fueling capacity
  - Capital, operating costs, and emission factor
- A set of transportation technologies, each is defined by:
  - The cargo (hydrogen, feedstock, or CO_2), and the transportation capacity
  - Capital, operating costs, and emission factor (for hydrogen transportation)

Determine

- The feedstock supply and CCS system
  - Which nodes are selected as feedstock supply sites
  - What type of feedstock does each selected node supply and in what quantity
  - Which nodes are selected to build the CO_2 storage sites
  - The processing rate of each storage site
- The installation and operation of hydrogen facilities
  - The number, location, size, and technology of production plants and fueling stations
  - Whether the network runs on gaseous or liquid hydrogen
  - Whether a CCS system is employed at each production plant
  - The production rate and fueling rate
- The operation of the transportation technology
  - The rate of transportation of each type of cargo (hydrogen, feedstock, and CO_2) via each transportation mode between all locations

Subject to

- Feedstock availability, the maximum capacity of technologies (production, fueling, CO_2 processing, and transportation), and the satisfaction of all fixed-location demand and a given percent of FCEV's demand.

In order to

- Minimize the least cost of hydrogen (LCOH), which includes the contribution of capital investment, feedstock purchase, operating cost, and emission cost.

From a system modeling viewpoint, the hydrogen supply network design falls within the general category of strategic supply chain management problems (Mula et al., 2010). In terms of the structural features of the supply chain, the proposed model is a single-commodity (hydrogen), mono-period, deterministic model with four location layers (feedstock, production, fueling station, and CO_2 storage). In addition to the typical location-allocation decisions, this model also involves decisions related to capacity, production, and transportation modes.

4. Mathematical model

Sets

$e \in E$	feedstock types
$f \in F$	transportation mode of feedstock
$h \in H$	transportation mode of hydrogen
$i \in I$	hydrogen physical forms
$j \in J$	fueling facility sizes
$k \in K$	production facility sizes
$n, m \in N$	nodes
N_q	nodes on shortest path of OD (Origin–Destination) pair q
$o \in O$	on-site fueling technologies
$p \in P$	production technologies
$q \in Q$	OD (Origin–Destination) flow pairs
$s \in S$	standard fueling technologies

Subsets

$(e, f) \in EF \subseteq E \times F$	combinations of feedstock types and transportation modes
$(e, o) \in EO \subseteq E \times O$	combinations of feedstock types and on-site fueling technologies
$(e, p) \in EP \subseteq E \times P$	combinations of feedstock types and production technologies
$(i, h) \in IH \subseteq I \times H$	combinations of hydrogen physical forms and transportation modes

Considering the problem characteristics, a MILP model is developed. The model assumptions are shown below. The objective function and constraints are characterized subsequently.

4.1. Model assumptions

The study is based on the following assumptions:

- The length of the shortest path between each pair of nodes is regarded as the distance between the two nodes, which is given as input data;
- Two types of fixed-location demand are considered: Type A refers to stationary applications such as combined heat and power system, and Type B refers to fleet vehicles. For the former, one needs only to deliver the required amount of hydrogen, while for the latter, in addition to meeting the fixed-location demand, one should also build a standard fueling station to satisfy the fueling demand at that node;
- The vehicles required to deliver hydrogen and feedstock are rented;
- The potential locations where the CO_2 storage sites could be built are given as model inputs;

- Only the CO_2 emission of the hydrogen production plants could be captured and processed by the CCS system;
- The total amount of CO_2 emission of the HSCN could be zero or negative depending on the type of feedstock selected and whether a CCS system is adopted (e.g., when biomass is selected as feedstock and a CCS system is also applied). Negative emissions generate revenue. For simplicity, the carbon price remains the same for both positive and negative emissions.

4.2. Objective function

The optimization framework seeks to minimize the least cost of hydrogen ($LCOH$) in €/kg H_2, which is attained by dividing the total daily cost (TDC) by the amount of hydrogen delivered per day (THD):

$$Minimize \quad LCOH \tag{1}$$

$$LCOH = \frac{TDC}{THD} \tag{2}$$

The total daily cost (TDC) consists of the contribution of capital cost (CC), feedstock purchasing cost (EC), operating cost (OC), and emission cost (EMC):

$$TDC = CC + EC + OC + EMC \tag{3}$$

The amount of hydrogen delivered per day (THD) is given by

$$THD = \sum_{q} f_q^{pair} * IC_q + \sum_{n,i} (dem_{ni}^{h,A} + dem_{ni}^{h,B}) \tag{4}$$

The first term on the right-hand-side of Eq. (4) refers to the hydrogen demand of FCEVs, where f_q^{pair} is the amount of hydrogen fueling demand flow of OD (Origin–Destination) flow pair q, and IC_q equals 1 if flow pair q is captured. The second term refers to the fixed-location demand, and $dem_{ni}^{h,A}$ and $dem_{ni}^{h,B}$ represent the fixed demand at node n (in hydrogen form i) of Type A and Type B, respectively.

4.2.1. Daily capital cost (CC)

The capital cost is composed of facility capital cost (FCC) and CO_2 transportation capital cost (TCC):

$$CC = \frac{1}{\alpha * \beta}(FCC + TCC) \tag{5}$$

The right-hand-side of Eq. (5) is divided by the annual network operating period (α) and the payback period of capital investment (β) to find the cost per day.

- Facility capital cost (FCC)

$$FCC = \sum_{p,i,k} NP_{pik} * pcc_{pik} + \sum_{s,i,j} NF_{sij} * fcc_{sij} + \sum_{o,j} NF_{oj} * fcc_{oj} + NR * ccc \tag{6}$$

where NP_{pik} represents the number of production plants of technology p, hydrogen form i, and size k. pcc_{pik} is the capital cost of one plant of this type. NF_{sij} denotes the number of standard fueling stations of technology s, hydrogen form i, and size k. fcc_{sij} is the capital cost of one station of this type. NF_{oj} gives the number of on-site fueling stations of technology o and size j. fcc_{oj} is the capital cost of one station of this type. NR represents the number of CO_2 storage sites and ccc is the capital cost of one site.

- CO_2 transportation capital cost (TCC)

The TCC is obtained by multiplying the unit capital cost of CO_2 pipeline ($cpcc$) by the pipeline length:

$$TCC = cpcc * \sum_{n,m} X_{nm} * l_{nm} \tag{7}$$

where X_{nm} equals 1 if CO_2 is transported from node n to m, and l_{nm} is the shortest distance between the two nodes.

4.2.2. Daily feedstock purchasing cost (EC)

$$EC = \sum_{e} ESR_e * euc_e \tag{8}$$

where euc_e is the unit cost of the feedstock of type e, and ESR_e is the total supply rate of the feedstock of type e, given by

$$ESR_e = \sum_{n} (PESR_{ne} + OESR_{ne}) \tag{9}$$

where $PESR_{ne}$ is the supply rate of a feedstock site at node n that supplies feedstock of type e to hydrogen production plants (plants at the same node or built at other nodes). $OESR_{ne}$ is the feedstock supply rate of a feedstock site at node n that supplies feedstock of type e only to the on-site fueling station built at the same node.

4.2.3. Daily operating cost (OC)

The operating cost (OC) includes the facility operating cost (FOC), the operating cost associated with hydrogen, and feedstock transportation ($HTOC, FTOC$):

$$OC = FOC + HTOC + FTOC \tag{10}$$

- Facility operating cost (FOC)

$$FOC = \sum_{e} NE_e * eoc_e + \sum_{p,i,k} PR_{pik} * poc_{pik} + \sum_{s,i,j} FR_{sij} * foc_{sij} + \sum_{o,j} FR_{oj} * foc_{oj} + CR * coc \tag{11}$$

where NE_e represents the number of feedstock supply sites that supply feedstock of type e to hydrogen production plants. eoc_e is the operating cost of one site of this type. PR_{pik} gives the total production rate of the production plants of technology p, hydrogen form i, and size k. poc_{pik} is the unit operating cost (per kg H_2) of this type of plant. FR_{sij} denotes the total fueling rate of standard fueling stations of technology s, hydrogen form i, and size j. foc_{sij} is the unit operating cost (per kg H_2) of this type of station. FR_{oj} represents the total fueling rate of on-site fueling stations of technology o and size j. foc_{oj} is the unit operating cost (per kg H_2) of this type of station. CR gives the total processing rate of CO_2. coc is the unit operating cost (per kg CO_2).

- Hydrogen transportation operating cost ($HTOC$)

$$HTOC = HFC + HLC + HMC + HGC + HRC \tag{12}$$

the five items on the right-hand-side are the fuel cost, labor cost, maintenance cost, general cost, and vehicle rental cost of hydrogen transportation, respectively. They are defined in Eqs. (13) - (17):

$$HFC = \sum_{h,n,m} fp_h * \frac{2 * l_{nm} * Q_{hnm}}{fe_h * tcap_h} \tag{13}$$

$$HLC = \sum_{h,n,m} dw_h * \frac{Q_{hnm}}{tcap_h} * (\frac{2 * l_{nm}}{sp_h} + lut_h) \tag{14}$$

$$HMC = \sum_{h,n,m} me_h * \frac{2 * l_{nm} * Q_{hnm}}{tcap_h} \tag{15}$$

$$HGC = \sum_{h,n,m} ge_h * \frac{Q_{hnm}}{tma_h * tcap_h} * (\frac{2 * l_{nm}}{sp_h} + lut_h) \tag{16}$$

$$HRC = \sum_{h} NV_h * tcr_h \tag{17}$$

In these equations, fp_h, dw_h, me_h, ge_h, and tcr_h represent the fuel price (per liter fuel), driver wage (per hour), maintenance expense (per km), general expense (per day), and vehicle rental cost (per vehicle) of hydrogen transportation mode h, respectively. fe_h, sp_h, $tcap_h$, tma_h, and lut_h denote the fuel economy, speed, capacity, availability (hours per day), and load/unload time of hydrogen transportation mode h, respectively. Q_{hnm} represents the hydrogen transportation flux (in mode h) from node n to m, and l_{nm} is the shortest distance between the two nodes. NV_h denotes the number of hydrogen transportation vehicles of mode h and is calculated by the following:

$$NV_h \geqslant \sum_{n,m} \frac{Q_{hnm}}{tma_h * tcap_h} * (\frac{2 * l_{nm}}{sp_h} + lut_h), \quad \forall h \in H \tag{18}$$

- Feedstock transportation operating cost ($FTOC$)

$$FTOC = FFC + FLC + FMC + FGC + FRC \tag{19}$$

The five items on the right-hand-side are the fuel cost, labor cost, maintenance cost, general cost, and vehicle rental cost of feedstock transportation, respectively. Their definitions have the same forms as those of the hydrogen transportation operating cost (Eqs. (13) - (17)).

4.2.4. Daily emission cost (EMC)

$$EMC = ER * cp \tag{20}$$

where cp is the carbon price and ER is the total emission rate, which is given by

$$ER = (PER - PER^c) + SFER + OFER + TER \tag{21}$$

PER is the production emission rate, which is obtained by

$$PER = \sum_{n,p,i,k} PR_{npik} * (\gamma^{eu}_{pik} + \gamma^{eo}_{pik}) \tag{22}$$

In the equation, PR_{npik} denotes the production rate of a production plant of technology p, hydrogen form i, and size k. γ^{eu}_{pik} and γ^{eo}_{pik} are the production upstream and on-site emission factors of this type of plant, respectively.

PER^c is the total emission rate of production plants where emissions are processed, given by

$$PER^c = \sum_{n} PER^c_n \tag{23}$$

where PER_n^c is the emission rate of a production plant at node n, where emissions are processed, given by

$$PER_n^c = \sum_{p,i,k} PR_{npik}^c * \gamma_{pik}^{eo} * \gamma_{pik}^c \tag{24}$$

where PR_{npik}^c represents the production rate of a production plant of technology p, hydrogen form i, and size k, and where emissions are processed (see Eq. (65)), and γ_{pik}^c is the production emission capture efficiency of this type of plant.

Fueling emission rates are obtained by Eqs. (25) and (26):

$$SFER = \sum_{s,i,j} FR_{sij} * \gamma_{sij}^e \tag{25}$$

$$OFER = \sum_{o,j} FR_{oj} * \gamma_{oj}^e \tag{26}$$

$SFER$ and $OFER$ are the total emission rates of the standard and on-site fueling stations, respectively. FR_{sij} represents the total fueling rate of standard fueling stations of technology s, hydrogen form i, and size j. γ_{sij}^e is the emission factor of this type of station. FR_{oj} denotes the total fueling rate of on-site fueling stations of technology o and size j. γ_{oj}^e is the emission factor of this type of station.

The emission rates related to hydrogen transportation (TER) depend on fuel usage, given by

$$TER = \sum_{h,n,m} \gamma_h^e * \frac{2 * l_{nm} * Q_{hnm}}{fe_h * tcap_h} \tag{27}$$

where γ_h^e is the emission factor of hydrogen transportation, which represents the volume of emissions due to the unit fuel usage. Q_{hnm} represents the hydrogen transportation flux (in mode h) from node n to m, and l_{nm} is the shortest distance between the two nodes. fe_h and $tcap_h$ are the fuel economy and capacity of hydrogen transportation mode h. The emissions results from feedstock transportation are included in the upstream emission of hydrogen production, therefore do not need to be calculated separately.

4.3. Constraints

4.3.1. Mass balance constraints

- Hydrogen

The hydrogen mass balance is defined at each node n, and for each hydrogen form i, such that the hydrogen production (PR_{npik}) and input from other nodes m (Q_{hmn}) meets the fueling demand (FR_{nsij}), the fixed-location demand ($dem_{ni}^{h,A}, dem_{ni}^{h,B}$) of this node n, and the hydrogen output to

other nodes m (Q_{hnm}), as follows:

$$\sum_{p,k} PR_{npik} + \sum_{\substack{m \\ h:(i,h)\in IH}} Q_{hmn} = \sum_{\substack{m \\ h:(i,h)\in IH}} Q_{hnm} + \sum_{s,j} FR_{nsij} + dem_{ni}^{h,A} + dem_{ni}^{h,B}, \quad \forall n \in N, i \in I \tag{28}$$

- Feedstock

For feedstock consumed by hydrogen production plants, the feedstock mass balance is defined at each node n, for each combination of feedstock types and production technologies (e, p), such that the feedstock supply ($PESR_{ne}$) and input from other nodes m (Q_{fmn}) meets the consumption of feedstock, which is calculated by multiplying the production rate at that node (PR_{npik}) by the corresponding conversion rate ($\delta_{(e,p)}$), and the feedstock output to other nodes m (Q_{fnm}), as follows:

$$PESR_{ne} + \sum_{\substack{m, \\ f:(e,f)\in EF}} Q_{fmn} = \sum_{\substack{m, \\ f:(e,f)\in EF}} Q_{fnm} + \sum_{i,k} PR_{npik} * \delta_{(e,p)}, \quad \forall n \in N, (e,p) \in EP \tag{29}$$

For feedstock consumed by on-site fueling stations, the feedstock mass balance is given:

$$OESR_{ne} = \sum_{j} FR_{noj} * \delta_{(e,o)}, \quad \forall n \in N, (e,o) \in EF \tag{30}$$

In the equation, $OESR_{ne}$ represents the feedstock supply rate. FR_{noj} denotes the fueling rate and $\delta_{(e,o)}$ is the conversion rate of feedstock (type e) to hydrogen at on-site stations.

- CO_2

The CO_2 mass balance should be likewise satisfied at each node n to quantify the infrastructure needs for a CCS system.

$$PER_n^c + \sum_{m} Q_{mn} = \sum_{m} Q_{nm} + CR_n, \quad \forall n \in N \tag{31}$$

In the equation, PER_n^c represents the emission rate of a production plant at node n, where emissions are processed. Q_{mn} is the CO_2 transportation flux from node m to n, whereas Q_{nm} is the flux from node n to m. CR_n is the CO_2 processing rate.

4.3.2. Feedstock constraints

The feedstock supply rate ($PESR_{ne}$, $OESR_{ne}$) cannot exceed certain limits:

$$IE_{ne} * ecap_{ne}^{min} \leqslant PESR_{ne} \leqslant IE_{ne} * ecap_{ne}^{max}, \quad \forall n \in N, e \in E \tag{32}$$

$$IF_{no} * ecap_{ne}^{min} \leqslant OESR_{ne} \leqslant IF_{no} * ecap_{ne}^{max}, \quad \forall n \in N, (e,o) \in EO \tag{33}$$

$$PESR_{ne} + OESR_{ne} \leqslant ecap_{ne}^{max}, \quad \forall n \in N, e \in E \tag{34}$$

IF_{no} equals 1 if there is an on-site fueling station of technology o at node n, and is defined by

$$IF_{no} = \sum_{j} IF_{noj}, \quad \forall n \in N, o \in O \tag{35}$$

The number of feedstock supply sites that supply feedstock of type e to hydrogen production plants (NE_e) is defined as

$$NE_e = \sum_{n} IE_{ne} \tag{36}$$

In Eqs. (32) - (36), IE_{ne} equals 1 if node n is chosen as a feedstock supplier (type e) of production sites. IF_{noj} equals 1 if there is an on-site fueling station of technology o and size j at node n. The bounds of feedstock supply capacity are denoted by *ecap*.

4.3.3. Production constraints

The production rate (PR_{npik}) cannot exceed certain limits:

$$IP_{npik} * pcap_{pik}^{min} \leqslant PR_{npik} \leqslant IP_{npik} * pcap_{pik}^{max}, \quad \forall n \in N, p \in P, i \in I, j \in K \tag{37}$$

The number of production plants (NP_{pik}) is given by

$$NP_{pik} = \sum_{n} IP_{npik} \tag{38}$$

The total production rate of production plants (PR_{pik}) is defined as

$$PR_{pik} = \sum_{n} PR_{npik} \tag{39}$$

In Eqs. (37) - (39), IP_{npik} equals 1 if there is a production plant at node n, of technology p, hydrogen form i, and size k. The bounds of production capacity are represented by *pcap*.

4.3.4. Fueling station constraints

The fueling rate (FR_{nsij}, FR_{noj}) cannot exceed certain limits:

$$IF_{nsij} * fcap_{sij}^{min} \leqslant FR_{nsij} \leqslant IF_{nsij} * fcap_{sij}^{max}, \quad \forall n \in N, s \in S, i \in I, j \in J \tag{40}$$

$$IF_{noj} * fcap_{oj}^{min} \leqslant FR_{noj} \leqslant IF_{noj} * fcap_{oj}^{max}, \quad \forall n \in N, o \in O, j \in J \tag{41}$$

The total fueling rates (FR_{sij}, FR_{oj}) are defined as

$$FR_{sij} = \sum_{n} FR_{nsij} \tag{42}$$

$$FR_{oj} = \sum_{n} FR_{noj} \tag{43}$$

The number of fueling stations (NF_{sij}, NF_{oj}) are given by

$$NF_{sij} = \sum_{n} IF_{nsij} \tag{44}$$

$$NF_{oj} = \sum_{n} IF_{noj} \tag{45}$$

In Eqs. (40) - (45), IF_{nsij} equals 1 if there is a standard fueling station at node n, of technology s, hydrogen form i, and size j. IF_{noj} equals 1 if there is an on-site fueling station at node n, of technology o and size j. The bounds of fueling capacity are denoted by $fcap$.

If fixed-location hydrogen demand of Type B exists at node n (means $id_n^{h,B}$ equals 1), a standard fueling station should also be built at this node:

$$SIF_n \geqslant id_n^{h,B}, \quad \forall n \in N \tag{46}$$

SIF_n equals 1 if there is a standard fueling station at node n.

4.3.5. Transportation constraints

The transportation flux of hydrogen, feedstock, and CO_2 (Q_{hnm}, Q_{fnm}, Q_{nm}) cannot exceed certain limits:

$$X_{hnm} * tcap_h^{min} \leqslant Q_{hnm} \leqslant X_{hnm} * tcap_h^{max}, \quad \forall h \in H, n, m \in N \tag{47}$$

$$X_{fnm} * tcap_f^{min} \leqslant Q_{fnm} \leqslant X_{fnm} * tcap_f^{max}, \quad \forall f \in F, n, m \in N \tag{48}$$

$$X_{nm} * tcap^{min} \leqslant Q_{nm} \leqslant X_{nm} * tcap^{max}, \quad \forall n, m \in N \tag{49}$$

In Eqs. (47) - (49), X_{hnm}, X_{fnm}, and X_{nm} are binary variables that take the value of 1 if transportation links are established from node n to m. The bounds of transportation capacity are represented by $tcap$.

Transportation between different nodes can only occur in one direction:

$$X_{hnm} + X_{hmn} \leqslant 1, \quad \forall h \in H, n, m \in N \tag{50}$$

$$X_{fnm} + X_{fmn} \leqslant 1, \quad \forall f \in F, n, m \in N \tag{51}$$

$$X_{nm} + X_{mn} \leqslant 1, \quad \forall n, m \in N \tag{52}$$

A node can only export hydrogen when there is a production plant at this node:

$$IP_n \geqslant X_{hnm}, \quad \forall h \in H, n, m \in N \tag{53}$$

where IP_n equals 1 if there is a production plant (of any technology, any hydrogen form, and any size) at this node. The following equation ensures that only one plant could be installed at each node.

$$IP_n = \sum_{p,i,k} IP_{npik}, \quad \forall n \in N \tag{54}$$

where IP_{npik} equals 1 if there is a production plant at node n, of technology p, hydrogen form i, and size k.

Hydrogen is imported into the nodes that have standard fueling stations or fixed-location demand of Type A, or both:

$$SIF_n + id_n^{h,A} \geqslant X_{hmn}, \quad \forall h \in H, n, m \in N \tag{55}$$

where SIF_n equals 1 if there is a standard fueling station (of any technology, any hydrogen form, and any size) at this node. $id_n^{h,A}$ indicates whether node n has fixed-location demand of Type A.

A node cannot export feedstock when there is no feedstock supplier of hydrogen production plants (of any type of feedstocks) at this node (implies IE_n equals to 0):

$$IE_n \geqslant X_{fnm}, \quad \forall f \in F, n, m \in N \tag{56}$$

where IE_n is defined as

$$IE_n = \sum_e IE_{ne}, \quad \forall n \in N \tag{57}$$

where IE_{ne} equals 1 if node n is chosen as a feedstock supplier that supplies feedstock of type e to production plants.

The end of the feedstock transportation link can only be the production plants:

$$IP_n \geqslant X_{fmn}, \quad \forall f \in F, n, m \in N \tag{58}$$

where IP_n equals 1 if there is a production plant at node n.

A node can only export CO_2 when the emission of the production plant at this node is processed (means IM_n equals 1):

$$IM_n \geqslant X_{nm}, \quad \forall n, m \in N \tag{59}$$

The CO_2 transportation link ends only at the nodes where CO_2 storage sites are located (means IR_n equals 1):

$$IR_n \geqslant X_{mn}, \quad \forall n, m \in N \tag{60}$$

4.3.6. Emission constraints

The production emission of a node cannot be processed if there is no plant at this node:

$$IM_n \leqslant IP_n, \quad \forall n \in N \tag{61}$$

where IP_n denotes whether node n has a production plant, and IM_n takes the value of 1 if the emission of the plant at that node is processed.

The CO_2 processing rate (CR_n) cannot exceed certain limits:

$$IR_n * ccap_n^{min} \leqslant CR_n \leqslant IR_n * ccap_n^{max}, \quad \forall n \in N \tag{62}$$

where IR_n equals 1 if there is a CO_2 storage site at node n. The bounds of CO_2 processing capacity are represented by *ccap*.

The total processing rate of CO_2 (CR) is given by

$$CR = \sum_n CR_n \tag{63}$$

where CR_n is the CO_2 processing rate of a CO_2 storage site at node n.

The number of CO_2 storage sites (NR) is defined as

$$NR = \sum_{n} IR_n \tag{64}$$

The production rate of a production plant where emissions are processed (PR^c_{npik}) can be obtained by the following equation:

$$PR^c_{npik} = IM_n * PR_{npik}, \quad \forall n \in N, p \in P, i \in I, k \in K \tag{65}$$

where PR_{npik} represents the production rate of a production plant at node n, and IM_n denotes whether the emission of this plant is processed.

The Eq. (65) is nonlinear and can be linearized by the following constraints:

$$PR^c_{npik} \leqslant IM_n * pcap^{max}_{pik}, \quad \forall n \in N, p \in P, i \in I, k \in K \tag{66}$$

$$PR^c_{npik} \leqslant PR_{npik}, \quad \forall n \in N, p \in P, i \in I, k \in K \tag{67}$$

$$PR^c_{npik} \geqslant PR_{npik} - (1 - IM_n) * pcap^{max}_{pik}, \quad \forall n \in N, p \in P, i \in I, k \in K \tag{68}$$

where $pcap^{max}_{pik}$ is the upper limit of production capacity.

4.3.7. Demand constraints

The percentage of hydrogen fueling demand flow that can be captured ($DEM^{h,cap}$) should be equal to the number given as input ($dem^{h,exp}$):

$$DEM^{h,cap} = dem^{h,exp} \tag{69}$$

Because hydrogen fueling demand flow of OD (Origin–Destination) flow pairs are discrete values, the following constraints to replace the Eq. (69) are introduced:

$$dem^{h,exp} \leqslant DEM^{h,cap} \leqslant dem^{h,exp} + \epsilon \tag{70}$$

where ϵ is a small positive number, which is set to 0.01 in this study, and $DEM^{h,cap}$ is defined by

$$DEM^{h,cap} = \frac{\sum_q f^{pair}_q * IC_q}{\sum_q f^{pair}_q} * 100 \tag{71}$$

where f^{pair}_q is the amount of hydrogen fueling demand flow of OD flow pair q, and IC_q equals 1 if flow pair q is captured.

A hydrogen fueling demand flow is captured if there is at least one fueling station (of any technology and any size) on one of the nodes that lie on the shortest path of this flow pair:

$$\sum_{n \in N_q} IF_n \geqslant IC_q, \quad \forall q \in Q, \tag{72}$$

where IF_n equals 1 if there is a fueling station (standard or on-site) at this node. The following equations ensure that only one fueling station could be installed at each node.

$$IF_n = SIF_n + OIF_n, \quad \forall n \in N \tag{73}$$

$$SIF_n = \sum_{s,i,j} IF_{nsij}, \quad \forall n \in N \tag{74}$$

$$OIF_n = \sum_{o,j} IF_{noj}, \quad \forall n \in N \tag{75}$$

where SIF_n equals 1 if there is a standard fueling station at node n, and OIF_n equals 1 if there is an on-site fueling station at this node. IF_{nsij} equals 1 if there is a standard fueling station at node n, of technology s, hydrogen form i, and size j. IF_{noj} equals 1 if there is an on-site fueling station at node n, of technology o and size j.

The fueling rate at node n (FR_{nsij}, FR_{noj}) should be able to cover the amount of hydrogen fueling demand flow captured by the fueling station established at that node:

$$\sum_{s,i,j} FR_{nsij} \geqslant SIF_n * f_n^{node}, \quad \forall n \in N \tag{76}$$

$$\sum_{o,j} FR_{noj} \geqslant OIF_n * f_n^{node}, \quad \forall n \in N \tag{77}$$

where f_n^{node} is the hydrogen fueling demand flow of node n.

5. Case study: Franche-Comté, France

The developed model is applied to Franche-Comté, a region of eastern France (since 2016, it is part of the new region Bourgogne-Franche-Comté.). Its total area is 16,202 km^2. In 2016, its population was 1,180,397 persons.

5.1. Network description

The 31 most populous cities are selected as network nodes. Demographic data of each city are collected based on the *commune*[1] in which the city is located. The most populous city is

[1]The commune is a level of administrative division in France.

Besançon, the capital of the region. There are several large cities in the northeast, including Belfort, Montbéliard and Valentigney. Other major cities include Vesoul in the north, Dole in the west, and Pontarlier in the south. The main roads (including auto-routes, national roads, and departmental roads) connecting the cities are selected as network edges. There are 65 edges. Length data are acquired from Google Maps^{TM}. The length of the network's edges and the distances between different cities are given in the supplementary material. The network generated is presented in Fig. 2 - (a).

Three types of feedstock are considered in this study: natural gas, electricity, and biomass. Natural gas can be supplied only in cities that are covered by the natural gas network. According to GRTgaz (2017, 2019)[2], 23 cities have access to the natural gas network, as shown in Fig. 2 - (b). The maximum supply capacity of natural gas is fixed at 30,000 Nm^3/d. Electricity is available in all cities (see Fig. 2 - (c)). The maximum supply capacity is fixed at 300,000 kWh/d. It is assumed that two cities (Luxeuil-les-Bains in the north and Valdahon in the center) could supply biomass, and the maximum supply capacity is fixed at 70,000 kg/d. The feedstock prices are shown in Table B.8.

It is assumed that a potential CO_2 storage site is located at Morteau and its maximum processing capacity is 200,000 kg CO_2/d (see Fig. 2 - (d)). Other CCS system inputs can be found in Table B.8. It is also assumed that the fixed-location demand of Type A exists at Saint-Claude, the amount of hydrogen demand is 500 kg/d. Fixed-location demand of Type B exists at Pontarlier, the amount of demand is 500 kg/d (see Fig. 2 - (e)).

5.2. Hydrogen fueling demand

The proposed model satisfies two major types of hydrogen demand: fixed-location demand (node-based) and fueling demand of FCEVs (flow-based). This section explains how the fueling demand of FCEVs is represented by the flow-based demand. The classical Flow-Capturing Location Model (FCLM) defines only the locations of the service facilities. Decision-makers receive no references on the required service capacity to satisfy part or all of the "flow captured". It is evident that the relationship between the "flow captured" and the service capacity should be built before the capacity-related decision variables are introduced into the model. In the context of fueling station deployment, such a relationship is often established between the fueling demand and the road traffic flow. The underlying assumption is that all units of traffic flow within the region (between different origins and destinations) contribute equally to the fueling demand. Considering most of the vehicles on the road still rely on gasoline or diesel, this assumption is reasonable when deploying traditional fueling stations. However, this same assumption becomes questionable when the problem has been changed to hydrogen fueling station planning. It is mainly due to uneven distribution of FCEVs within the region's traffic flow. Therefore, the concept of hydrogen fueling

[2]GRTgaz is a French natural gas transmission system operator.

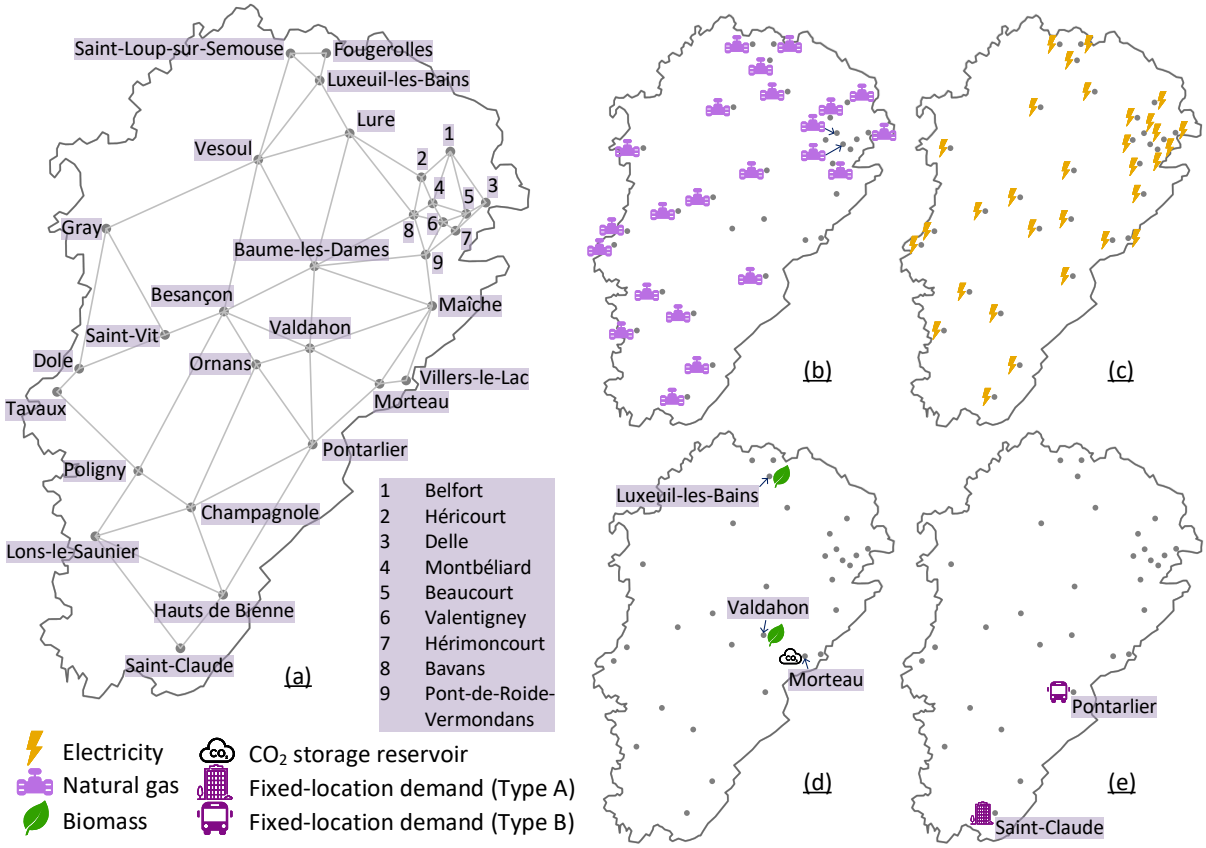

Figure 2: Franche-Comté network: (a) Basic network; (b) Natural gas distribution; (c) Electricity distribution; (d) Biomass distribution and location of a potential CO_2 storage site; (e) Location of fixed-location demands

demand flow is introduced, which is a modified traffic flow that involves the influences of potential FCEV owner-ships in different cities or towns. The fueling capacity of a hydrogen fueling station is therefore defined by the hydrogen fueling demand flow that has been captured by the station.

It is assumed that hydrogen fueling demand flow is more likely to appear between two closer cities with higher FCEV owner-ships. The potential FCEV ownership is related not only to the population but also to several demographic metrics. Melendez & Milbrandt (2008) proposed nine metrics that influence FCEV adoption by consumers. Given the availability of statistics, the following four are chosen for this study:

- *Vehicle*[3]*:* Households with multiple vehicles are more likely to adopt hydrogen vehicles.
- *Income*[4]*:* Higher incomes lead to earlier adoption of FCEV.

[3]The ratio of households with two or more vehicles.
[4]Yearly household income.

- *Education*[5]*:* Higher education leads to earlier adoption.
- *Commute*[6]*:* Commuting with private vehicles interests consumers in newer and more efficient vehicles.

Table B.1 provides the population size and four demographic metrics for each city. Data are collected from L'Institut national de la statistique et des études économiques (2015a,b, 2018a,b)[7].

Considering all five factors, a "scoring system" similar to the one used by Melendez & Milbrandt (2006) is employed. In the "scoring system", data in each column are first normalized in the range of 1-100 to compute the score of each city on each item:

$$Score_x = 1 + 99 * \frac{Value_x - Value_{min}}{Value_{max} - Value_{min}} \tag{78}$$

Then the final score of each city is obtained by a linear combination of the five obtained scores, as shown in Eq. (79). The weights are chosen according to the importance of each metric.

$$\begin{aligned} Score_{final} = Score_{Population} * 0.6 + Score_{Vehicle} * 0.1 + Score_{Income} * 0.1 \\ + Score_{Education} * 0.1 + Score_{Commute} * 0.1 \end{aligned} \tag{79}$$

The final score represents the relative potential FCEV ownership of each city. If one considers the final score as the *weight* of each city, then a network with weight values of cities could be obtained, as presented in Fig. 3 - (a). The radius of circles at nodes is visually proportional to these weights. The plot of Fig. 3 - (b) is the weighted network based only on population. It can be seen that after considering the influence of the four additional demographic metrics, some cities with smaller populations have gained greater weight. For example, Villers-le-lac has the highest score of "Income", Gray has the highest score of "Vehicle", and Bavans has higher scores in both "Vehicle" and "Commute". It can also be found that, although Besançon is still the city with the largest weight, the urban agglomerations in the northeast have gathered several cities with relatively high weights.

After computing the demand level for the 31 considered cities, the potential flow of FCEVs on the roads of the network should be determined. First, the gravity model (Haynes & Fotheringham, 1985) is used to quantitatively measure the possibility that an OD pair flow becomes a hydrogen fueling demand flow. As shown in Eq. (80), the possibility (P_q) of an OD pair (q) that links two cities n and m can be expressed as a ratio of the multiplied final scores (weights of cities obtained

[5]Share of persons whose highest degree is a bachelor's degree in the out-of-school population aged 15 or over.
[6]Share of persons who use private vehicles for commuting.
[7]National Institute of Statistics and Economic Studies

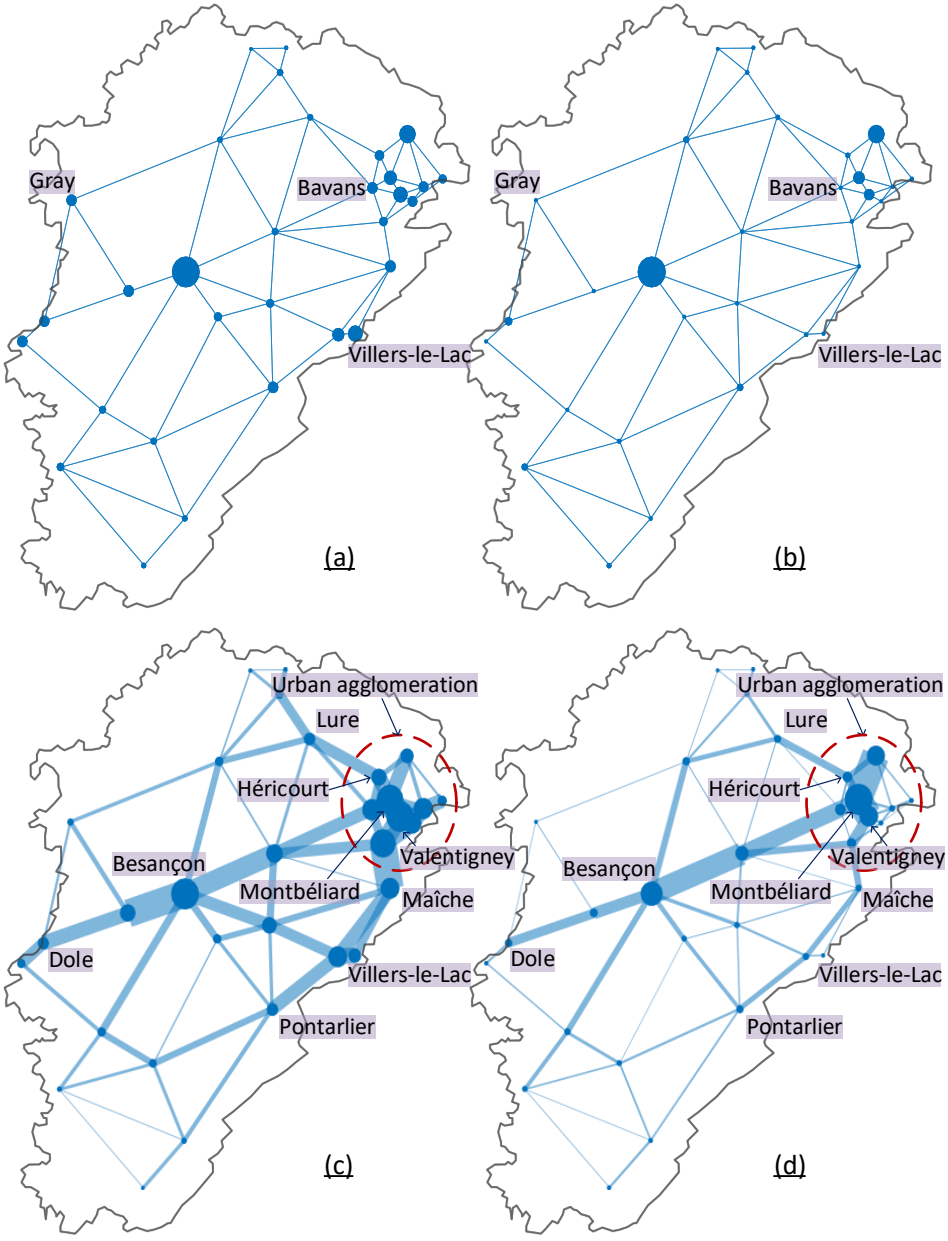

Figure 3: Hydrogen fueling demand flow: (a) Weighted network; (b) Weighted network based only on population; (c) Hydrogen fueling demand flow network; (d) Hydrogen fueling demand flow network based only on population

above) over the distance between any pair of cities.

$$P_q = \frac{Score_{final,city_n} * Score_{final,city_m}}{l_{nm}} \tag{80}$$

The obtained results can be regarded as "weights" of origin–destination (OD) pairs, with which

the value of hydrogen fueling demand flow of each pair is determined. Based on the report of L'Association Française pour l'Hydrogène et les Piles à Combustible (2018)[8], it is estimated that the potential hydrogen demand of FCEV in Franche-Comté in 2030 will be 4,378 kg/d[9]. This total demand is distributed to OD pairs according to their "weights" obtained by Eq. (80). In this way, the hydrogen fueling demand is linked to the OD flow pairs, and the resulting demand flow network is presented in Fig. 3 - (c). The larger the radius of the circle, the higher the fueling demand in the city. The wider the edge, the greater the fueling demand flow carried by that edge. Comparing this flow network with the one based only on population (Fig. 3 - (d)), the common element is the region's east-west traffic artery–A36 (Montbéliard-Besançon-Dole), which carries the largest hydrogen fueling demand in both networks. However, one observes the following differences:

- The hydrogen fueling demand flow between the eastern urban agglomerations has increased significantly. This can be explained as follows: According to the gravity model, greater weight and closer distance result in larger interaction. The urban agglomerations formed by several cities with large weights have reasonably more interactions with each other.

- In the east, the flow through Lure, Héricourt, Valentigney, Maîche, Pontarlier has increased significantly. This can be explained by the fact that small cities like Villers-le-lac, Maîche, and Bavans have higher weights.

5.3. Hydrogen supply network

5.3.1. Production plants

Corresponding to three types of feedstock, three types of production technologies are set up: steam methane reforming (SMR), electrolysis, and biomass gasification (BG). The production plant has three sizes (small, medium, and large), with production capacity ranging from 1,000 kg/d to 5,000 kg/d. Each type of plant has sets of data for the production of gaseous hydrogen and liquid hydrogen. Data are collected mainly from the Hydrogen Analysis (H2A) project conducted by the U.S. Department of Energy (Department of Energy, 2010, 2018b,c,d). Tables B.2, B.3, and B.4 present the capital cost, operating cost, production capacity, emission factor, and emission capture efficiency for each type of production technology. Attention has been directed to use the local emission factor of electricity that is obtained from the Électricité de France (2018)[10]. The conversion rates of production technologies can be found in Table B.8.

[8]The French Association for Hydrogen and Fuel Cells

[9]The report provides only the total hydrogen demand of FCEV in France in 2030 (89,000 kg/d). The value for Franche-Comté is obtained by multiplying the total demand with the proportion of province (Franche-Comté) population to France population (1.80% (L'Institut national de la statistique et des études économiques, 2015b))

[10]A French electric utility company

5.3.2. Fueling stations

The fueling capacity ranges from 50 kg/d to 1,200 kg/d, divided into four sizes - small, medium, large, and extra-large[11]. Standard fueling stations are divided into two subtypes according to the hydrogen form they receive, and the cost and emission data are shown in Table B.5. The on-site fueling stations consist of on-site-SMR and on-site-electrolysis. The cost and emission data are presented in Table B.6 (Melaina & Penev, 2013).

5.3.3. Hydrogen and feedstock transportation

Gaseous hydrogen is conveyed via tube trailers whereas liquefied hydrogen is transported in tanker trucks. For feedstock, this study considers only the transportation of biomass via trucks. The cost and emission data are presented in Table B.7.

5.4. Instances generation

One of the primary purposes of this study is to demonstrate the necessity of considering various components within a single framework. The influence of any component on the HSCN can be identified only by comparing and analyzing the model results with and without this component. Based on this principle, seven groups of instances have been designed, each of which corresponds to a component composition, as shown in Table 2.

Table 2: Groups of instances

	Model components				
	On-site station	Standard station	Feedstock transportation	CCS system	Fixed-location demand
Group A	✔				
Group B		✔			
Group C	✔	✔			
Group D		✔	✔		
Group E		✔		✔	
Group F		✔			✔
Group G	✔	✔	✔	✔	✔

- *Group A:* Only on-site stations are used to satisfy fueling needs. This can be seen as a simple upgrade of the classical FCLM (Flow-Capturing Location Model). The main mission is to locate on-site stations under the constraints of feedstock availabilities. In addition, the model needs to select a proper size for each on-site station.

- *Group B:* Only standard stations are employed to satisfy fueling needs. The model needs to locate standard stations as well as production plants, as the former can only receive hydrogen

[11] The fueling capacity of "extra-large" stations is twice that of "large" ones

produced by the latter. In this group of instances, feedstock transportation is forbidden. Therefore, a plant can use only the feedstock supplied by the city where it is located. Plants and standard stations are linked by hydrogen transportation. Group B integrates the HSCND model and the HFSP model, and covers the whole hydrogen supply chain, from feedstock to fueling stations.

- *Group C:* Based on Group B, with the addition of on-site stations. The introduction of on-site stations allows the model to choose between two completely different fueling technologies. It is reasonable to assume that "mix" may provide more interesting configurations. By comparing the results of instances of Group A, Group B, and Group C, one could learn how fueling technologies impact HSCN.

- *Group D:* Based on Group B, but allowing feedstock transportation. The introduction of feedstock transportation provides the model with the capability to examine the trade-off between the transportation of feedstock and hydrogen. By comparing the results of instances of Group B and Group D, one examines the necessity of integrating feedstock transportation into the model.

- *Group E:* Based on Group B, and involving a CCS system. Although the adoption of a CCS system could greatly reduce the CO_2 emission of HSCN, it yields huge expenses. The introduction of a CCS system makes the model capable of studying the trade-off between considerable emission costs and establishment of a CCS system. In addition, the model examines the trade-off among the transportation of hydrogen, feedstock, and CO_2 when locating production plants. By comparing the results of instances of Group B and Group E, one reviews the necessity of integrating a CCS system into the model.

- *Group F:* Based on Group B, adding fixed-location demand. The purpose of this group is to verify that the model can meet other hydrogen demand requirements while satisfying the fueling demands. By comparing the results of instances of Group B and Group F, one can observe how fixed-location demand changes the configuration of HSCN.

- *Group G:* All model components are involved. The model will be able to compare all possible configurations together and to consider various trade-offs to find the optimal result.

Within each group of instances, one or several sets are defined. The sets of a given group differ by the feedstock type or the hydrogen form, as shown in Table 3.

The model proposed in this study is mono-objective. The environmental impact of the HSCN is represented by the contribution of emission cost in the LCOH. Therefore, the value of the carbon price has a significant influence on the model results. Two levels of carbon price are set to observe the changes in configuration, especially the model's behavior toward a CCS system. Based on the

Table 3: Sets of instances within each group

	Feedstock			Hydrogen form	
	Electricity	Natural gas	Biomass	Gaseous	Liquid
Set A1	✔			N/A	N/A
Set A2		✔		N/A	N/A
Set B1		✔		✔	
Set B2		✔			✔
Set B3			✔	✔	
Set C		✔		✔	
Set D			✔	✔	
Set E1		✔		✔	
Set E2			✔	✔	
Set F		✔		✔	
Set G	✔	✔	✔	✔	✔

estimation of carbon price in Europe from various institutions (Carbon Tracker, 2018; Chestney, 2018; World Bank & Ecofys, 2018), the low level of carbon price (LC) is set to 0.05 €/kg CO_2, and the high level (HC) is set to 0.27 €/kg CO_2.

The potential hydrogen fueling demand is represented by "flow". It may not necessarily be "captured" totally. Decision-makers can decide freely the percent of flow that needs to be captured. For a specific percent of flow, the model provides the optimal HSCN configuration that satisfies these demands and the resulting LCOH. Fig. 4 presents the value of LCOH and number of fueling stations for each percent of flow captured of Set A1 with LC (low carbon price), from 1% to 100%. It can be seen that the LCOH curve appears U-shaped. A small fueling demand flow requires at least one station to be satisfied. Therefore, the contribution of capital cost to LCOH will be extremely high. Thus, for less than 10%, the smaller the percentage of flow captured, the higher the LCOH. At the other end, greater than 90%, the model needs to build more stations to approach 100%. This is because the places that are more efficient in flow capturing have already been chosen. The "extra" expenditure in capital cost causes the curve to rise sharply. For decision-makers, less than 10% and higher than 90% are areas of less interest. Therefore, three levels of fueling demand are set, 10% for low demand (LD), 50% for medium demand (MD), and 90% for high demand (HD). Then one can generate 66 instances. The name of each instance is formatted as "Set-N-C-D", where "N" is the name of 11 sets defined in Table 3, "C" is the carbon price level (LC or HC), and "D" represents the fueling demand level (LD, MD, or HD). Each instance is solved to obtain its value of LCOH and network configuration. Fig. 5 illustrates the configuration and captured hydrogen fueling demand flow of Set-A1-LC-MD. It is shown that three on-site stations are located at Besançon, Champagnole, and Valentigney. The captured flow is indicated in red. Based on the model's assumptions, a fueling station could capture all fueling demand of the node at which it is located. Correspondingly, all edges' flow directly linked to this node is also captured. This explains

why the three cities and their surrounding roads are all red. Flows in areas with no stations are less captured, as in the northern area. All instances analyzed in the following section have this kind of figure to provide a visual representation of the captured hydrogen fueling demand flow.

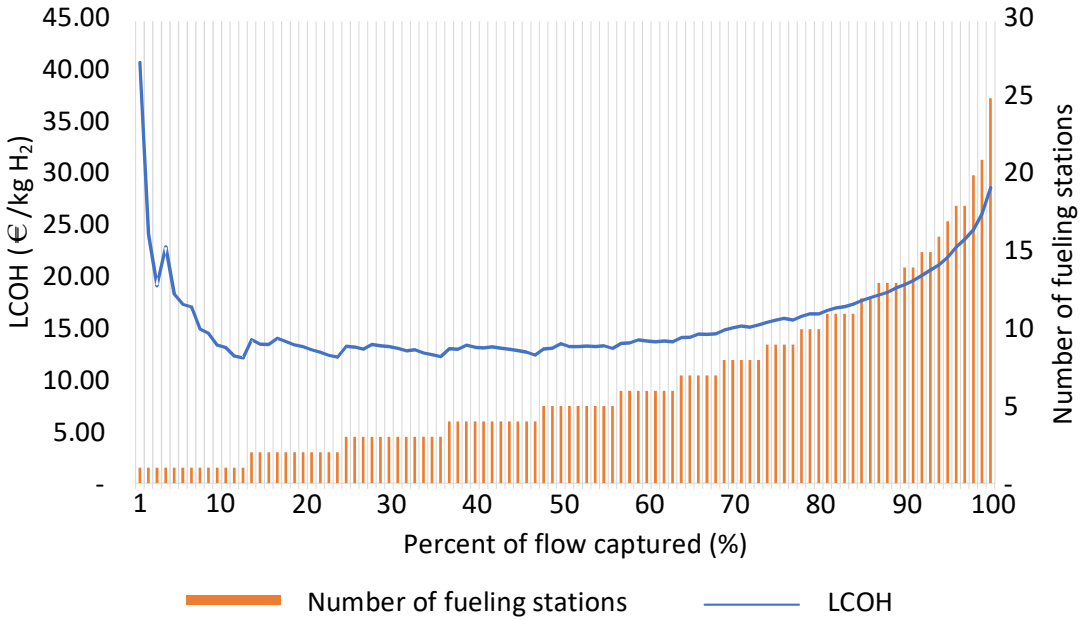

Figure 4: The value of LCOH and number of fueling stations for each percent of flow captured of Set A1 with LC (low carbon price), from 1% to 100%

6. Results and discussion

The model is solved by CPLEX 12.7 for the defined instances on a computer equipped with a 3.2 GHz i5-6500 and 16 GB of RAM. The corresponding computational statistics are summarized in Table 4. Fig. 6 provides a comparison of the results obtained in terms of LCOH. Detailed results of 66 instances are presented in the supplementary material.

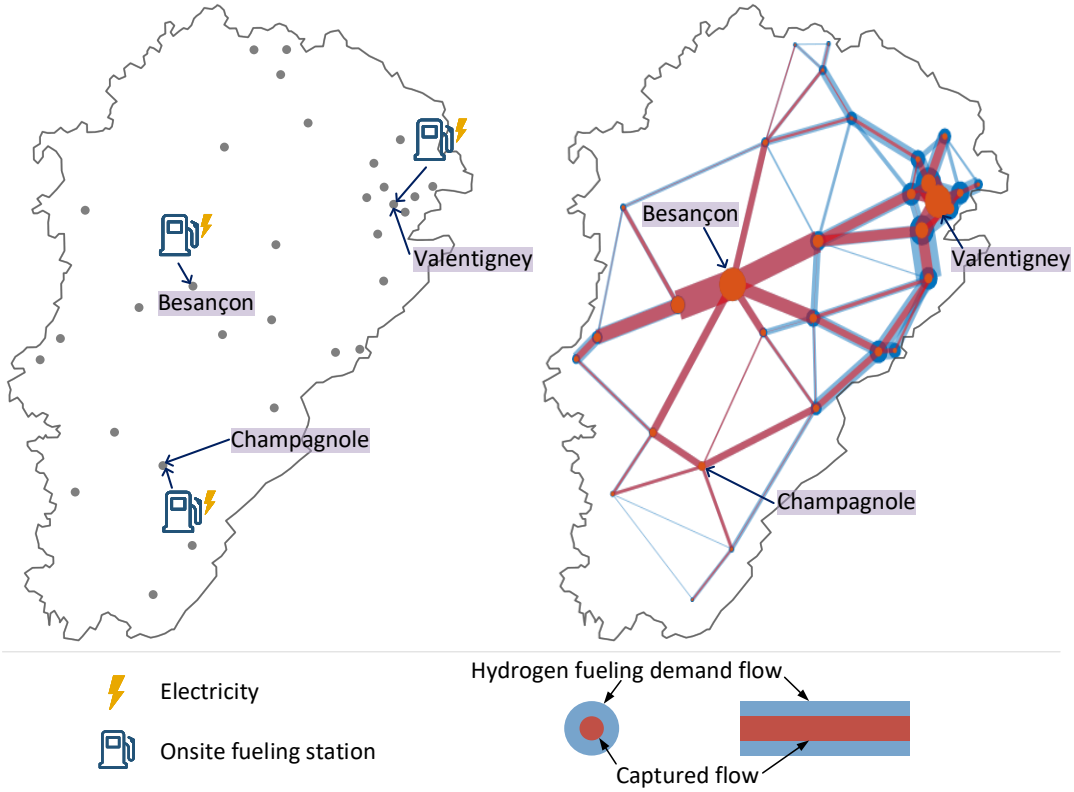

Figure 5: Configuration and captured hydrogen fueling demand flow of Set-A1-LC-MD

Table 4: Size of the instances

Instance group	A	B	C	D	E	F	G
Number of constraints	932	10,761	11,226	15,598	15,969	11,722	24,526
Number of binary variables	682	2,728	2,914	3,720	3,751	2,728	5,735
Number of integer variables	-	2	2	3	2	2	3
Number of continuous variables	155	2,170	2,325	3,131	3,255	2,170	5,673
Maximum CPU time (s)	1	7,567	16	407	144	11	539

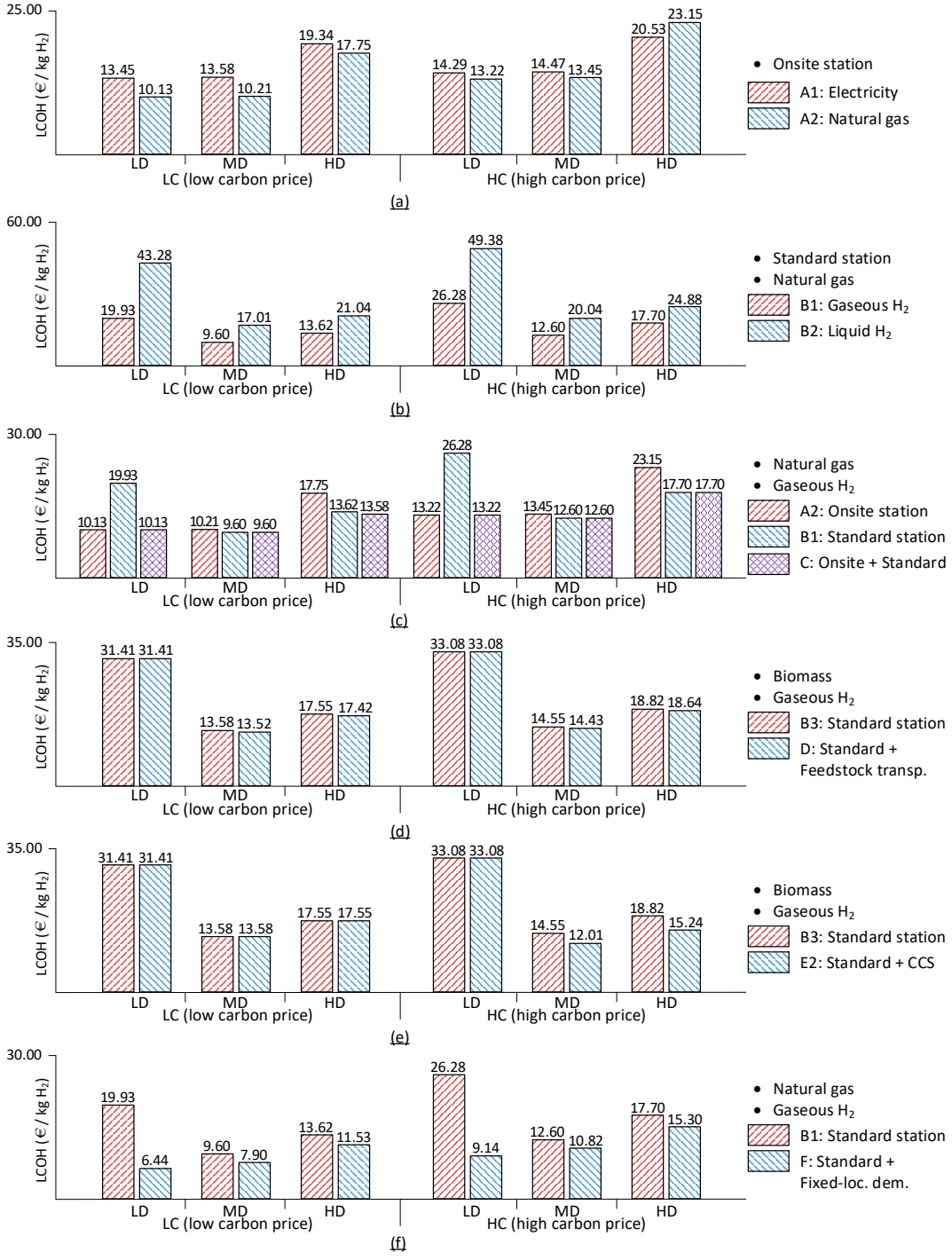

Figure 6: Obtained LCOH: (a) Set A1 vs. Set A2; (b) Set B1 vs. Set B2; (c) Set A2 vs. Set B1 vs. Set C; (d) Set B3 vs. Set D; (e) Set B3 vs. Set E2; (f) Set B1 vs. Set F

6.1. Role of feedstock availabilities

It is known that on-site-electrolysis stations have a higher capital cost than on-site-SMR, as shown in Table B.6. Therefore, in most situations, instances of Set A1 obtain a higher LCOH than instances of Set A2 (see Fig. 6 - (a)). As the emission factor of on-site-SMR is higher than that of on-site-electrolysis, the impact of emission costs will be more important as the carbon price is high. The gap between the two sets shrinks when carbon price increases, and this gap may even reverse for instances A_i-HC-HD.

Fig. 7 illustrates the differences between the supply chain structures obtained with the model for Set A1 and A2. Only the results for the high carbon price scenario are presented here. For the two sets of instances, one obtains the same number and locations of on-site stations at low and medium demands. It must be noted that Set A2 can only install on-site-SMR stations at cities that are covered by a natural gas network, which means that the model cannot locate stations considering only the efficiency of fueling demand flow capturing. Consequently, at high demand, Set A2 results in more stations and higher LCOH than Set A1.

6.2. Role of hydrogen forms

Fig. 6 - (b) shows that HSCN based on liquid hydrogen is more expensive at all three demand levels. The high cost is due to the need for liquefaction devices, which incur a high capital cost. Moreover, liquefaction requires a large amount of power consumption, increasing operating costs. Notice the gap between gaseous and liquid is shrinking when hydrogen demand rises. This can be explained by the advantage of liquid hydrogen in transportation. The number of vehicles required to transport the same amount of liquid hydrogen is smaller than for gaseous hydrogen because the capacity of a tanker truck (for liquid hydrogen) is nearly 23 times as large as a tube trailer (for gaseous hydrogen). Although the advantage in transportation cannot offset the high cost of liquefaction at low demand (i.e., when only a small number of vehicles are required), HSCN based on liquid hydrogen may be attractive when the demand of hydrogen increases.

In Fig. 8, one observes that, at medium and high demand, results for Set B2 involve fewer plants, and are more dependent on hydrogen transportation. This can reduce the disadvantages of high costs of liquefaction and take advantage of transportation. Therefore, it can be concluded that HSCN based on liquid hydrogen prefers centralized production.

6.3. Role of fueling technologies

First, observe Set A2 (on-site station only) and Set B1 (standard station only) in Fig. 6 - (c). It is shown that at low demand, Set B1 has higher LCOH. Indeed, any standard station requires to be supplied by a production plant, which increases the cost. At medium demand, the advantage of centralized production makes Set B1 reach lower LCOH than Set A2, and this advantage is even more obvious at high demand. The involvement of different fueling technologies provides the model

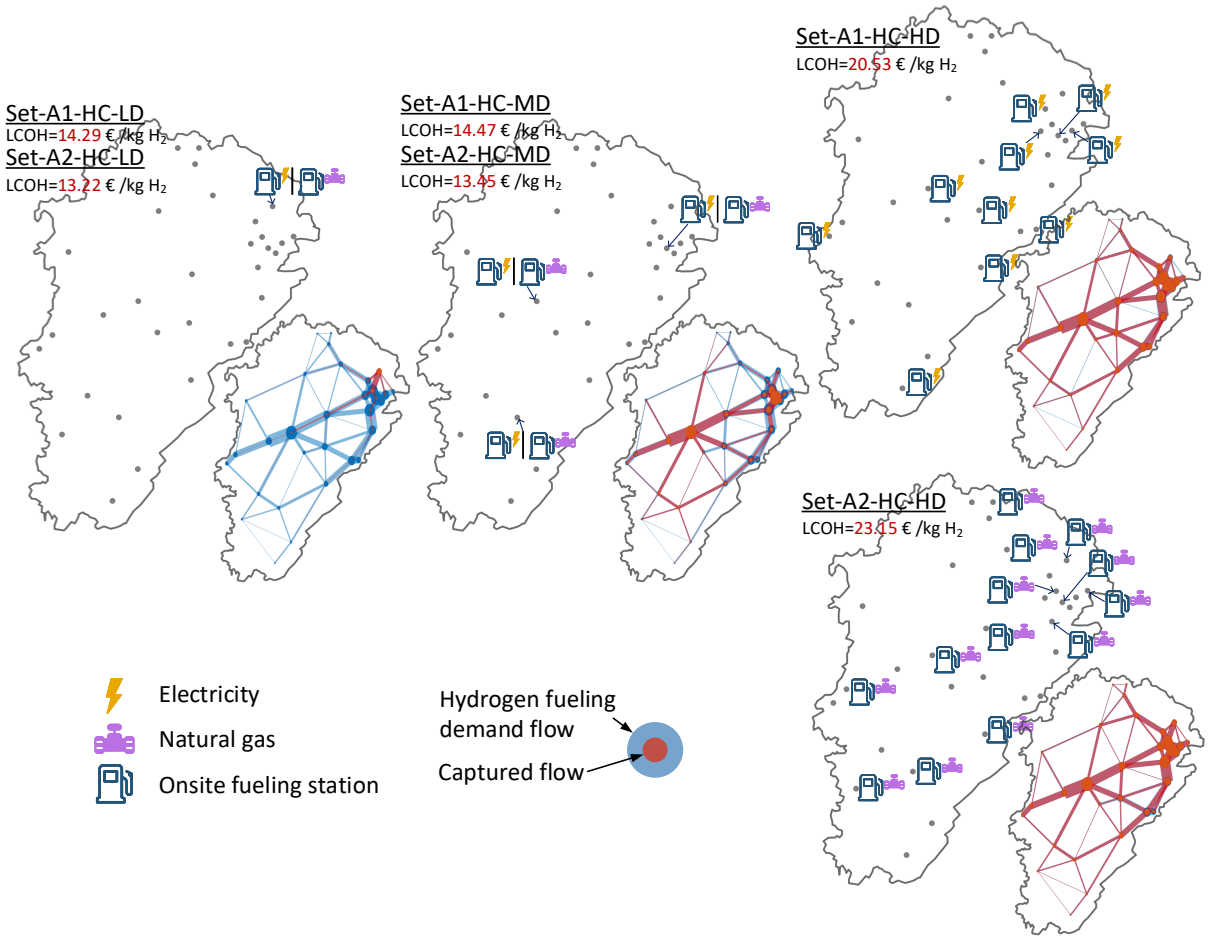

Figure 7: Configurations of Set A1 and A2 with high carbon price

with the ability to consider the trade-off between a centralized solution (with standard stations) and a decentralized configuration (with on-site stations).

It is reasonable to assume that "mix" could bring even better results (lower LCOH), and Set C is therefore introduced, as shown by the obtained solutions illustrated in Fig. 9. At low demand, Set C has the same configuration and LCOH as Set A2. At medium demand, Set C has the same results as Set B1. At high demand, Set C obtains the lowest LCOH. Although the instance Set-C-LC-HD has the same number of fueling stations as Set-B1-LC-HD, the former achieves lower LCOH by adopting both on-site and standard stations. In Set-C-LC-HD, the model chooses to install an on-site station at Champagnole. The introduction of an on-site station reduces the demand for hydrogen produced by production plants. Therefore Set-C-LC-HD has one less plant than Set-B1-LC-HD. Although these structural changes result in only a slight drop in LCOH, it proves that it is indeed possible to find a supply chain configuration with lower LCOH by allowing the model to consider both fueling technologies. Notice that in high carbon price scenarios, Set C

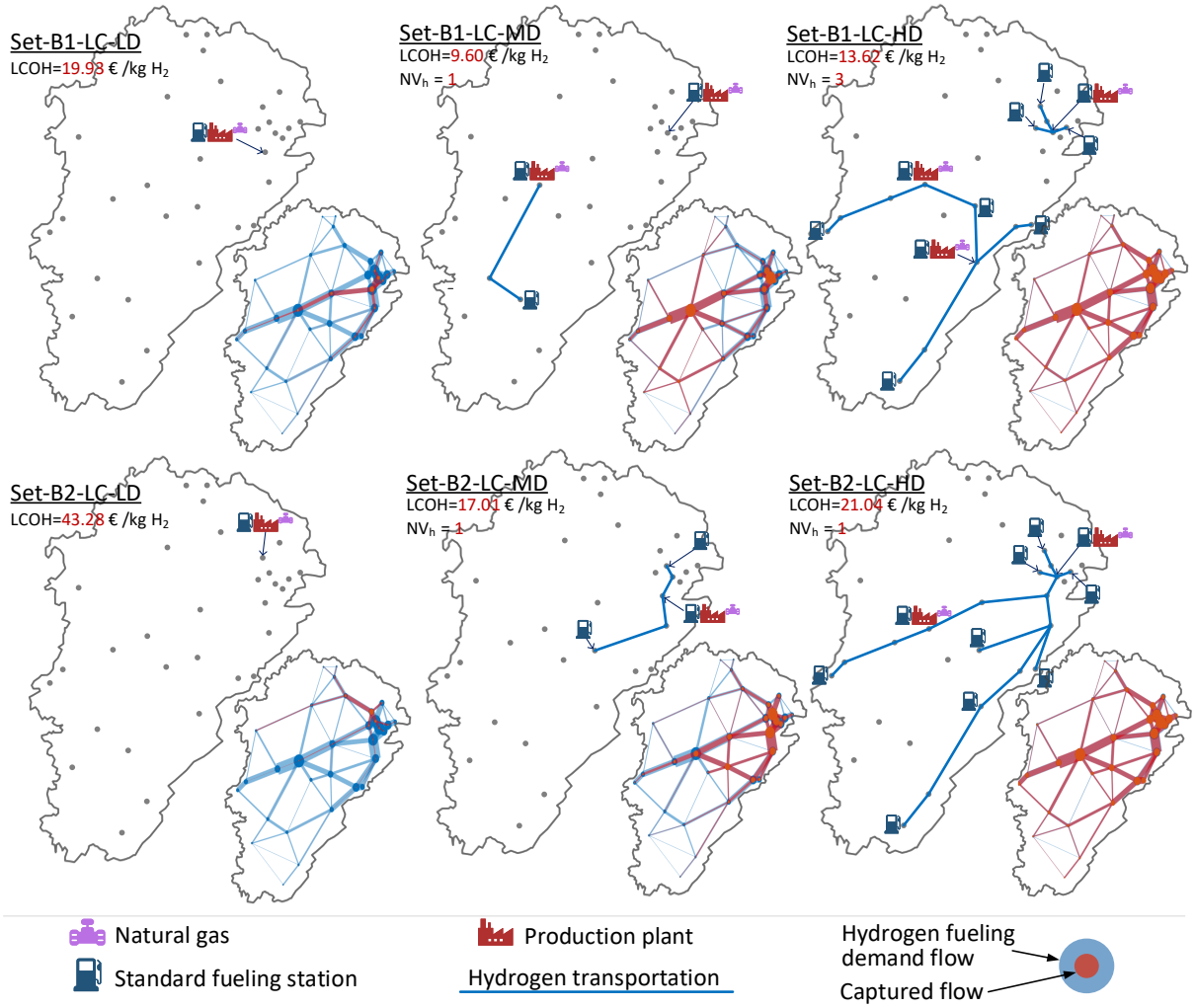

Figure 8: Configurations of Set B1 and B2 with low carbon price

and Set B1 have the same LCOH and configuration at high demand. The reason why Set C does not choose a "mix" solution in the high carbon price scenario can be explained by the fact that the emission factor of on-site-SMR is approximately seven times greater than the gaseous standard station emission factor. Therefore on-site stations are less attractive when carbon price rises.

6.4. Role of feedstock transportation

For this part, high carbon price does not bring changes in configuration (Fig. 6 - (d)). Only the results for low carbon price are discussed. Notice that at low demand, one obtains the same LCOH for Set D and B3. At medium and high demand, one obtains slightly different values of LCOH. That is because Set D uses feedstock transportation, and therefore finds lower LCOH. The comparison of Set-D-LC-HD and Set-B3-LC-HD serves as a good example to show how feedstock transportation

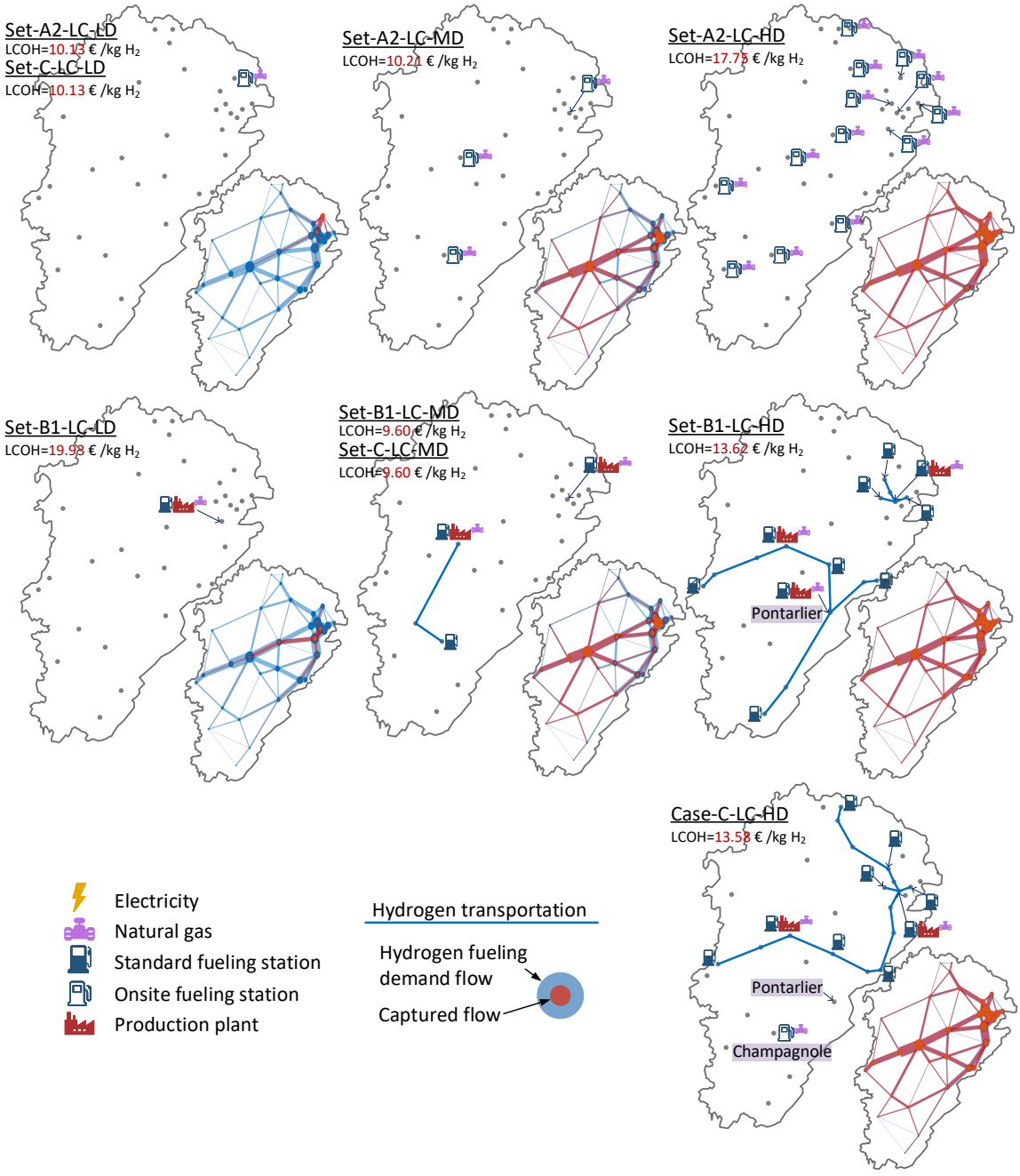

Figure 9: Configurations of Set A2, B1 and C with low carbon price

could help the model to find a better configuration (Fig. 10). Based on case input, biomass is supplied only at Luxeuil-les-Bains and Valdahon. In Set-B3-LC-HD, as feedstock transportation is not allowed, the model has to put two BG plants at the two cities. Notice that four fueling stations are located in the urban agglomerations in the northeast. It is reasonable to assume that

lower LCOH could be reached if the BG plant at Luxeuil-les-Bains is relocated within or near the urban agglomerations, and hydrogen transportation is replaced by feedstock transportation. This assumption is verified with the instance Set-D-LC-HD. For the two instances, one obtains the same number and locations of fueling stations. The change in LCOH results only from the involvement of feedstock transportation.

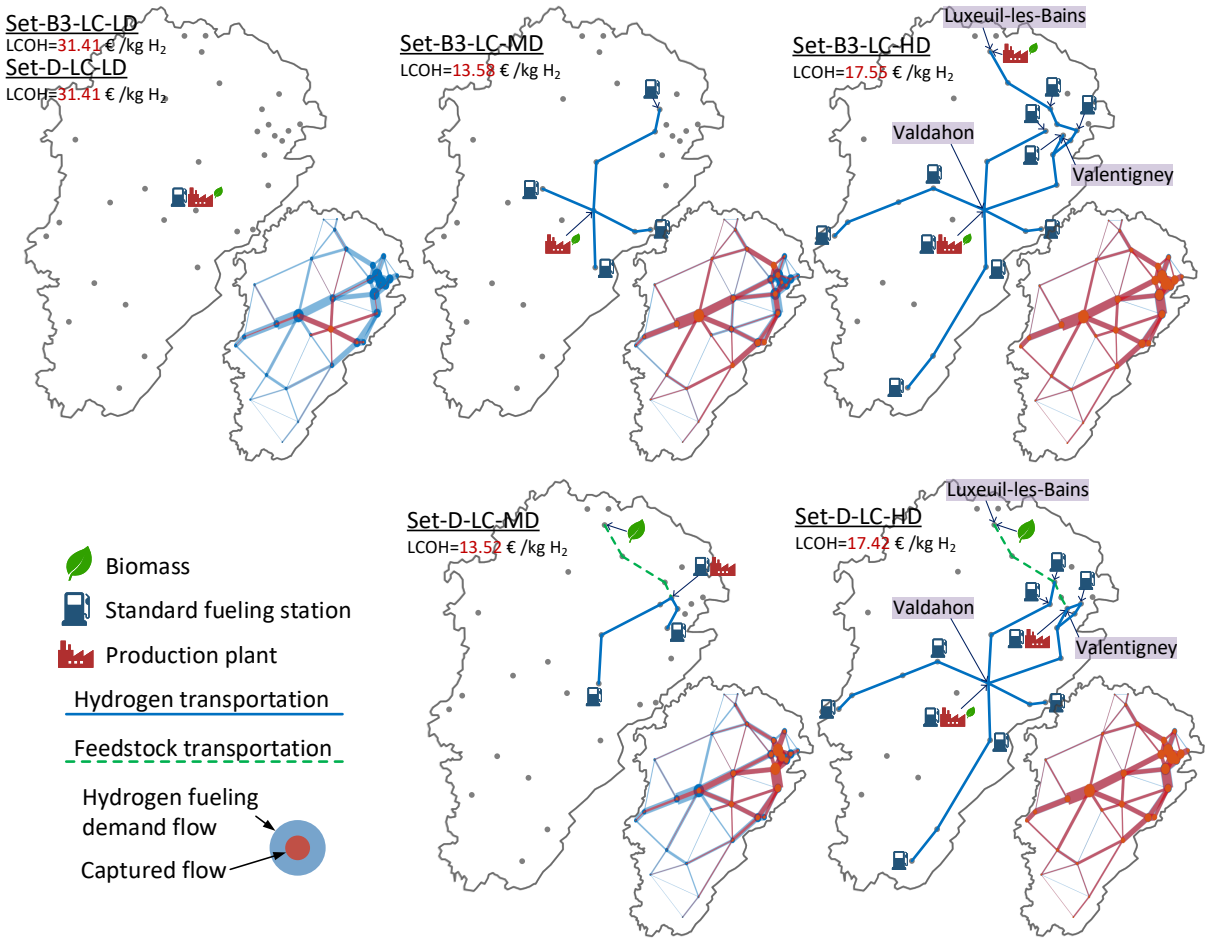

Figure 10: Configurations of Set B3 and D with low carbon price

6.5. Role of CCS system

Feedstock type and value of carbon price are two key factors that influence the choice of a CCS system. The optimal solution provided by the model does not include a CCS system in both low and high carbon price scenarios when natural gas is selected as feedstock (Set B1 vs. Set E1). It can be explained by the fact that the reduction in emission cost is not comparable to the expenses of a CCS system. The characteristic of biomass is that its upstream emission factor is negative. If a BG plant adopts a CCS system, 90% of its on-site emission will be captured so that the plant's CO_2

emissions are negative for every 1 kg of hydrogen produced using biomass. Hydrogen production plant emissions account for most of the total emissions of HSCN. Therefore, the entire system's emissions would likely be negative, and the system gains revenue because of negative emissions.

Fig. 6 - (e) provides obtained values of LCOH for Set B3 and E2. The model employs a CCS system only at medium and high demand in the high carbon price scenario. Analyzing the composition of LCOH shows that, although the adoption of a CCS system greatly increases the capital and operating costs, the negative emission reduces the overall cost, which makes the LCOH smaller. The obtained configurations are illustrated in Fig. 11. Notice that at high demand, only emission of the BG plant at Valdahon is captured, whereas emission of another BG plant at Luxeuil-les-Bains is not captured. This could be explained as Luxeuil-les-Bains is too far from Morteau, where the CO_2 storage site is located. If the model resulted in capturing emissions of the BG plant at Luxeuil-les-Bains, a 127 km CO_2 pipeline should be installed, adding a huge capital cost of 10.16 million euros. It can be concluded that a CCS system is attractive only at a high level of hydrogen demand and in high carbon price scenarios. Only when using biomass as feedstock, can benefits resulting from the reduction of emissions outweigh the huge expenses of adopting a CCS system.

Apart from carbon price, another leading strategy to promote CO_2 emission reductions is the maximum CO_2 emission constraint. The French government has set the carbon budget (CO_2 emission constraint) for the transport sector in 2029–2033 as 94 million metric tons per year (CO_2 equivalent) (Ministère de la Transition écologique et solidaire, 2018). Generally, the emission contributions of light duty vehicles (LDVs) account for 60% in the transport sector, which is 56.4 million metric tons per year in France. Multiplying this value with the proportion of province (Franche-Comté) population to France population (1.8%), one obtains the maximum emission of LDVs in Franche-Comté as 1 million metric tons per year. Assuming that the share of FCEVs in LDVs in Franche-Comté in 2030 is 2%, the maximum allowable emission limit for the HSCN designed in this study is 54,970 kg CO_2/d. A new parameter er^{max} is used to represent this upper bound and a new constraint is introduced:

$$ER \leqslant er^{max} \tag{81}$$

where ER is the total emission rate (kg CO_2/d) of the entire network.

The new constraint is imposed to Set E1 and E2 to observe the changes in network configuration under the simultaneous influences of carbon price and maximum emission constraint. It is found that configuration changes only occur in Set-E1-LC-HD and Set-E1-HC-HD. These two instances have the same ER (before the new constraint is applied) of 73,096 kg CO_2/d, which is larger than the maximum allowable emission limit. Fig. 12 illustrates these configuration changes. Notice that before the new constraint is introduced, Set-E1-LC-HD and Set-E1-HC-HD have the same configurations. They both have ten standard fueling stations and three production plants, located

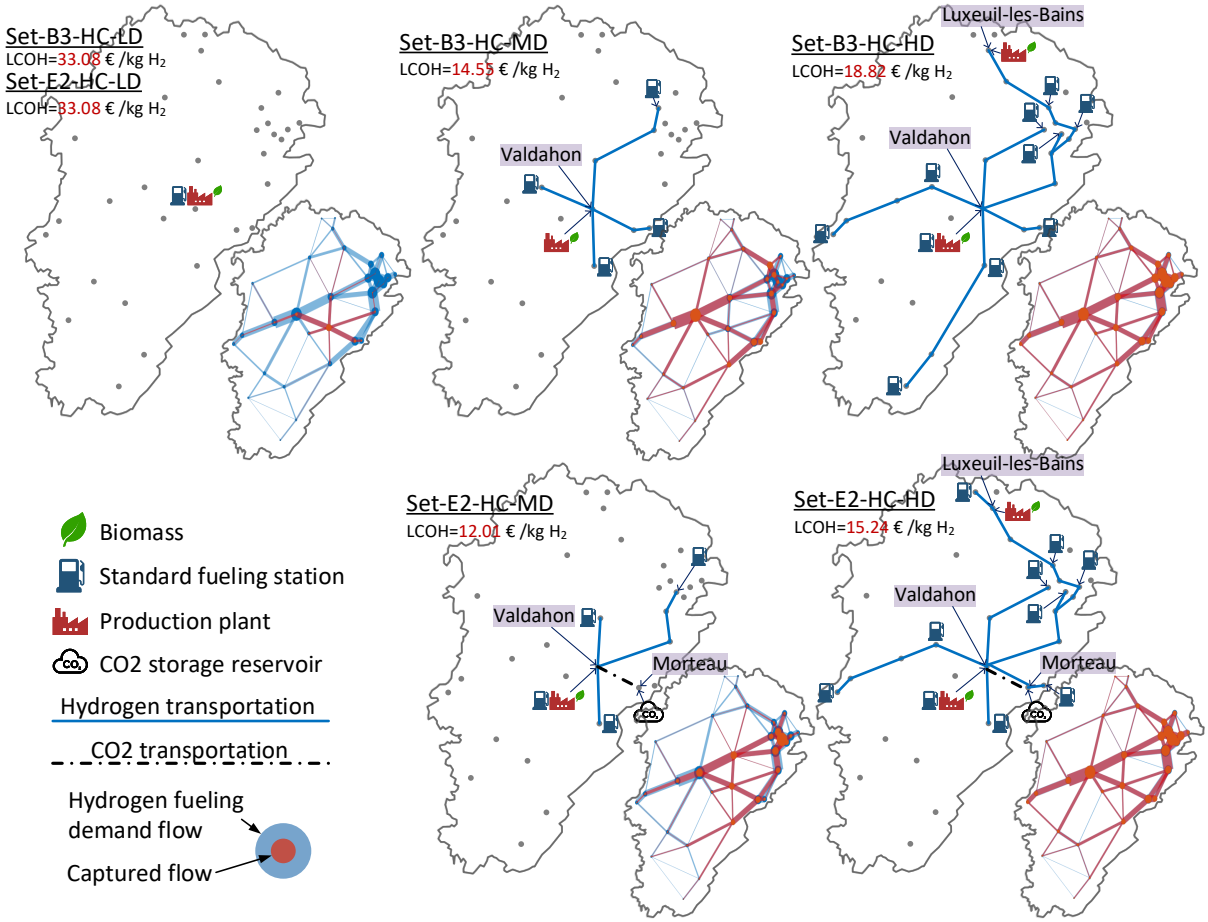

Figure 11: Configurations of Set B3 and E2 with high carbon price

in Besançon (production rate: 1,704 kg H_2/d), Valentigney (2,991 kg H_2/d), and Pontarlier (1,000 kg H_2/d). After the maximum emission constraint is applied, both instances adopt a CCS system. In addition, the production capacity has been re-deployed, and the hydrogen transportation has been re-organized. In the low carbon price scenario, the model chooses to capture the emission of the plant at Pontarlier. To capture sufficient emissions to reduce the total emissions below er^{max}, Besançon's plant has been closed, and its production capacity is transferred to the plant at Pontarlier. The reduction in the number of plants has made the system more dependent on hydrogen transportation, and the number of hydrogen transportation vehicles has increased from three to five. In the high carbon price scenario, the model chooses to capture even more emissions through centralized production. A large plant is located at Pont-de-Roide-Vermondans, where 49% of total emissions of the entire supply network are captured and processed. This value is only 28% in the low carbon price scenario. Although this results in long CO_2 pipeline distance (52 km compared to 29 km in the low carbon price scenario), the cost savings from further reduction

of emissions outweighs the increased capital cost. Based on this observation, it can be concluded that the maximum emission constraint forces instances where ER (before the new constraint is applied) is larger than er^{max} to adopt a CCS system. In the low carbon price scenario, the model only captures a small portion of emissions to satisfy the new constraint. In the high carbon price scenario, the model chooses to capture more emissions to reduce the carbon cost.

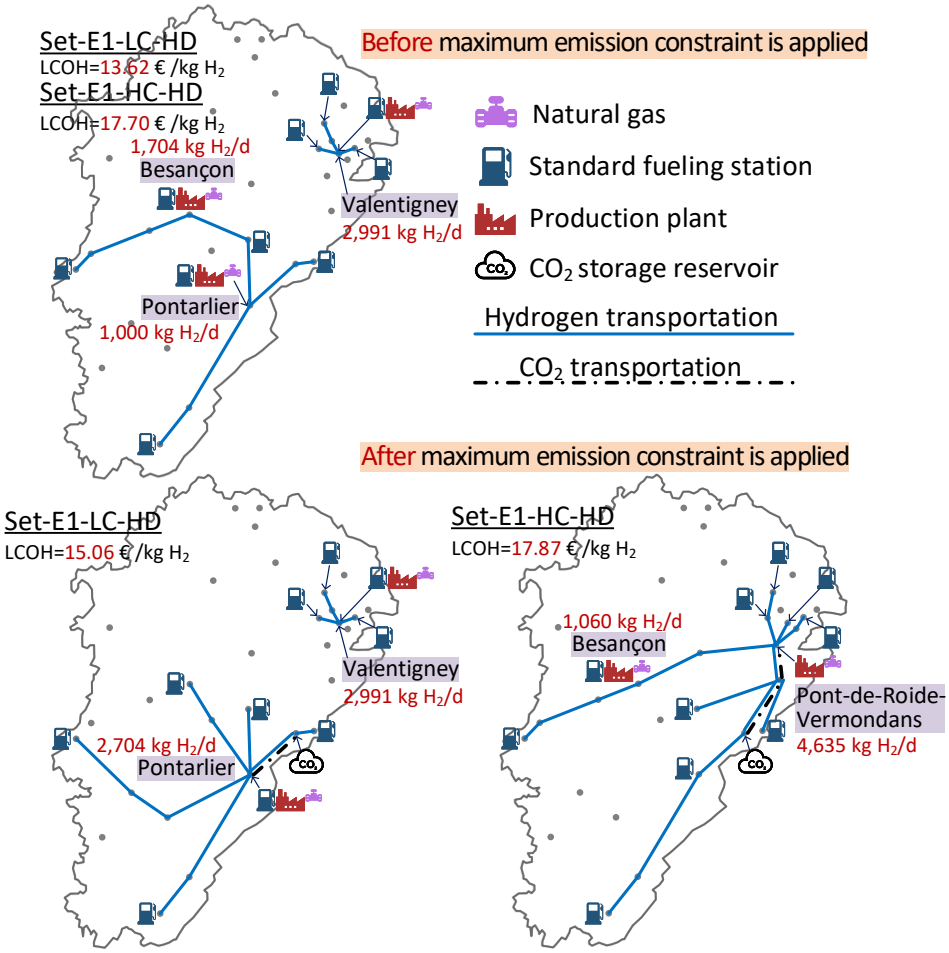

Figure 12: Configuration changes of Set-E1-LC(HC)-HD after the introduction of maximum emission constraint

6.6. Role of fixed-location demand

Fig. 13 shows the supply chain configurations provided by running the model with associated instances. To satisfy the fixed-location demand, instances in Set F have to build more facilities than those in Set B1. Take the medium-demand scenario as an example, Set B1 installs three fueling stations at three major cities - Valentigney, Besançon, and Champagnole, and two production plants at Valentigney and Besançon. Remember that fixed-location demands can be supplied only

by production plants. Set F builds a plant at Pontarlier, which facilitates the supply for fixed-location demand of Type A at Saint-Claude and fixed-location demand of Type B at Pontarlier. For Set F, a standard fueling station is installed at Pontarlier because there exists fixed-location demand of Type B. However, the fueling demand flow captured by this station is less than that of major cities. Therefore, the model has to build an additional station to capture 50% of fueling demand flow. Fig. 6 - (f) compares the values of LCOH for those two sets. Although the total daily cost for Set F is higher than Set B1, it obtains lower LCOH because a higher amount of hydrogen is sold.

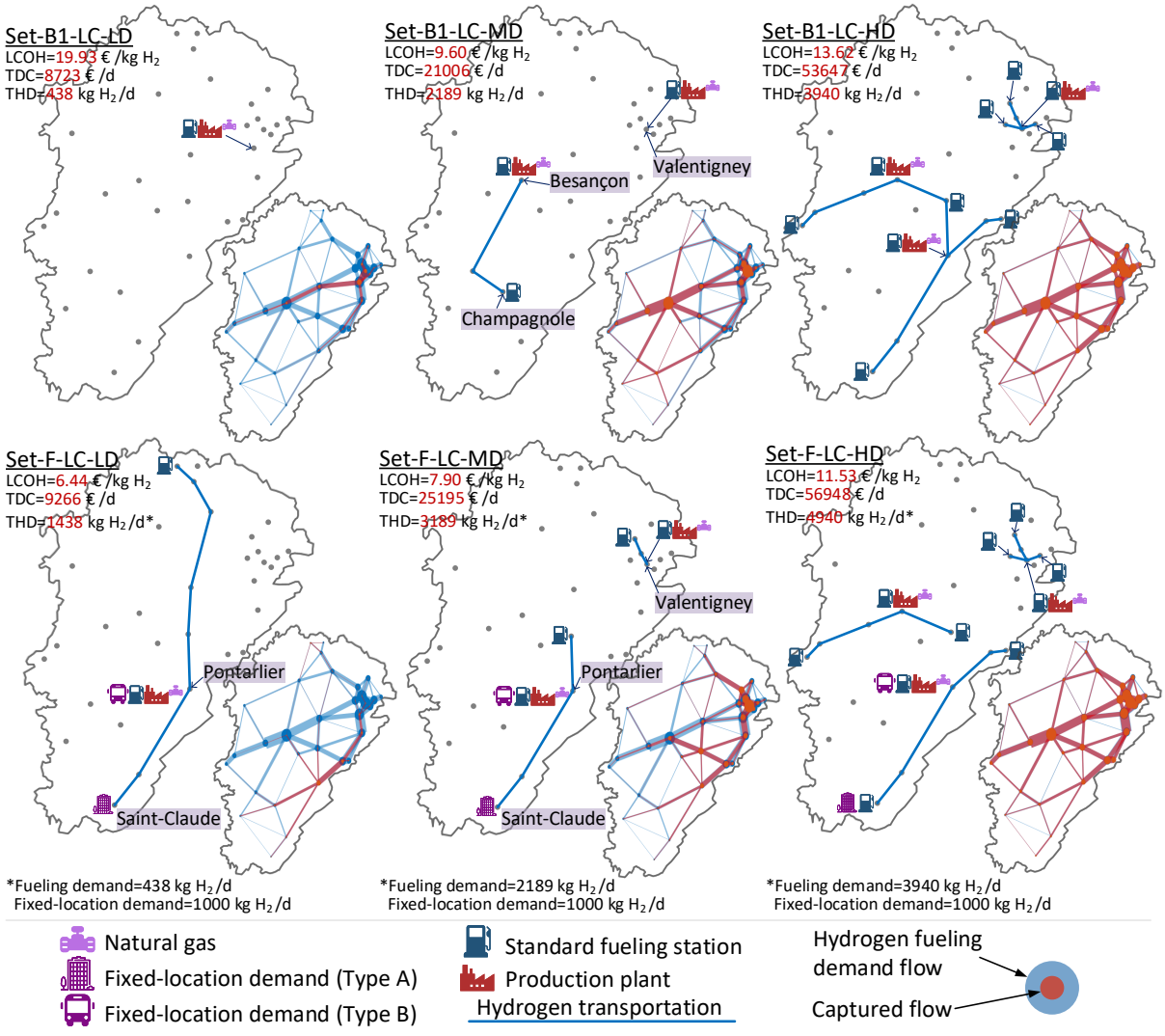

Figure 13: Configuration for Set B1 and F with low carbon price

6.7. The construction plan for Franche-Comté

Group G provides the complete instances in which all types of components are available to design the Franche-Comté hydrogen supply chain. Fig. 14 illustrates the configurations obtained in low and high carbon price scenarios. Notice that no on-site stations are installed in the presented configurations. This can be explained by the existence of fixed-location demand, which relies on hydrogen delivered by production plants. In the low carbon price scenario, the model selects SMR because production technology such as SMR plants are less expensive in capital cost, and the HSCN is built on gaseous hydrogen. The observed differences between the configurations of the two scenarios are that a CCS system has been adopted at medium and high demand and that BG plants are chosen instead of SMR plants. It is noteworthy that, CO_2 emissions of the two BG plants at high demand are all captured by the CCS system. The model chooses to install the two BG plants near the CO_2 storage site and accepts the long distances of feedstock transportation.

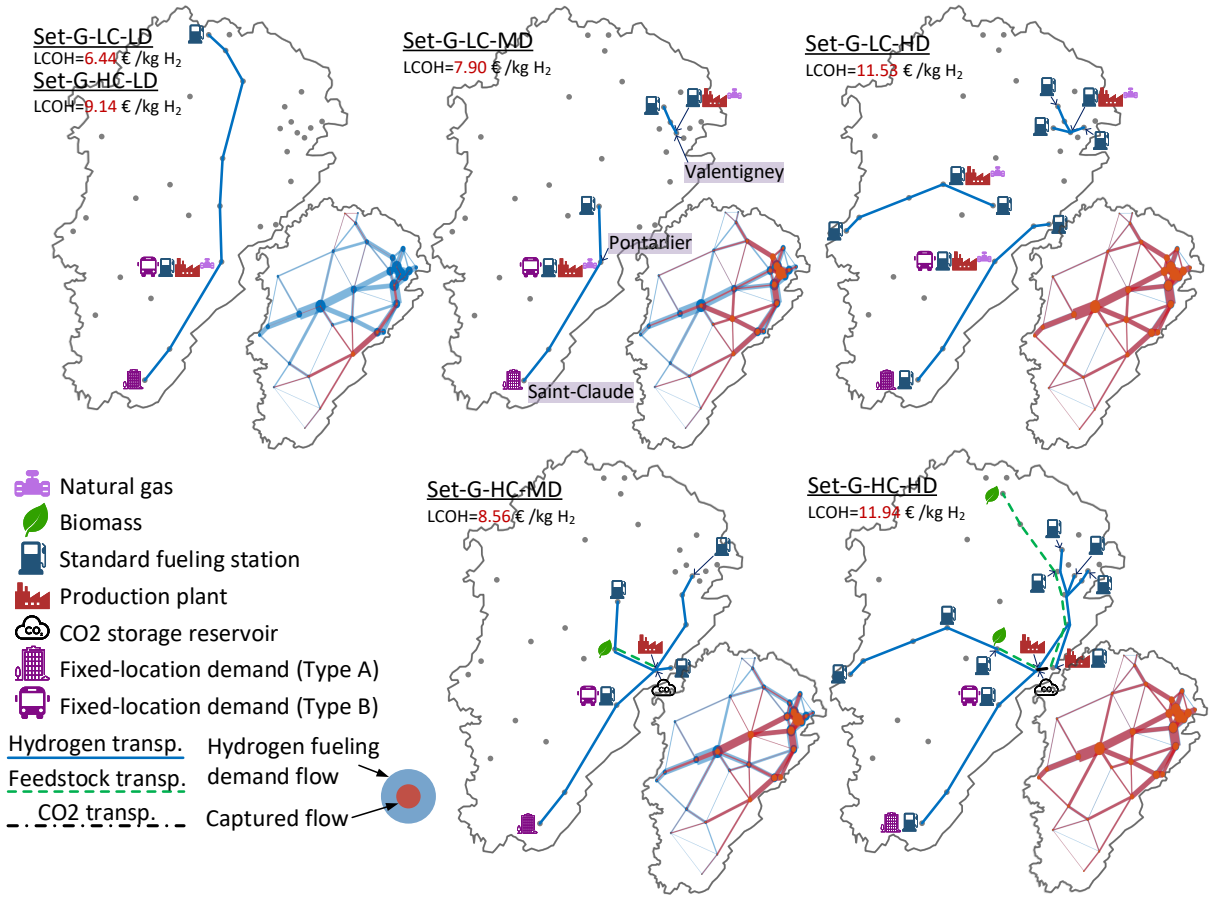

Figure 14: Configurations of Set G

7. Conclusion

The hydrogen supply chain network in the transportation sector is a complex system. It includes various components from feedstock supply sites to hydrogen fueling stations. Because of the inherent characteristics of a supply chain, each part of HSCN is interconnected rather than isolated. The selection of feedstock, production and fueling technology, locations of hydrogen facilities, and other major decisions make up a vast "pool" of pathways, each of which has a different value of LCOH and network configuration. For decision-makers, it is challenging to make intelligent designs without support from optimization models.

In this paper, a mathematical optimization model was developed, which integrates the hydrogen supply chain network design and hydrogen fueling station planning. Through the case study, it has been shown that first the model can provide an optimal supply configuration for a given set of available infrastructures. Second, thanks to the many comparisons made, the interest of the integrated model is highlighted, compared with others that consider only a subset of the components from feedstock supply sites to hydrogen fueling stations. Moreover, the approach conducted to validate the model consisted of executing it for each supply chain scenario considered. Therefore, it has also highlighted the potentially beneficial optimization-simulation coupling, which would consist of integrating this optimization model into a decision support system designed to simulate the various possible deployment scenarios.

At this stage, the computational results of the model are promising. However, there are major tasks that still need further investigation to improve it. The following tasks are summarized below:

- Consider the evolution of the HSCN over time, rather than a snapshot of the network at one point in time. In real-world conditions, the formation of the hydrogen energy market and the construction of the hydrogen energy supply network usually span decades. The hydrogen fueling demand increases gradually. Correspondingly, the construction plan of the HSCN should be designed in stages.

- Consider the interactions between the hydrogen supply (hydrogen facilities) and demand (FCEV potential buyers). In the present study, the hydrogen fueling demand flow is predefined, and it will not be affected by the hydrogen supply system. The influence of the hydrogen supply on demand has been ignored. The model will be improved by converting the hydrogen demand from model input to a decision variable to endogenously forecast hydrogen demand while optimizing the hydrogen supply network.

Acknowledgement

This work is financially supported by a program of the China Scholarship Council for Ph.D. Scholarship No. 201604490065.

References

Achtnicht, M., Bühler, G., & Hermeling, C. (2012). The impact of fuel availability on demand for alternative-fuel vehicles. *Transp. Res. Part D Transp. Environ.*, *17*, 262–269. doi:10.1016/J.TRD.2011.12.005.

Agnolucci, P., Akgul, O., McDowall, W., & Papageorgiou, L. G. (2013). The importance of economies of scale, transport costs and demand patterns in optimising hydrogen fuelling infrastructure: An exploration with SHIPMod (Spatial hydrogen infrastructure planning model). *Int. J. Hydrogen Energy*, *38*, 11189–11201. doi:10.1016/j.ijhydene.2013.06.071.

Agnolucci, P., & Mcdowall, W. (2013). Designing future hydrogen infrastructure: Insights from analysis at different spatial scales. *Int. J. Hydrogen Energy*, *38*, 5181–5191. doi:10.1016/j.ijhydene.2013.02.042.

Almansoori, A., & Betancourt-Torcat, A. (2016). Design of optimization model for a hydrogen supply chain under emission constraints - A case study of Germany. *Energy*, *111*, 414–429. doi:10.1016/j.energy.2016.05.123.

Almansoori, A., & Shah, N. (2006). Design and operation of a future hydrogen supply chain: Snapshot model. *Chem. Eng. Res. Des.*, *84*, 423–438. doi:10.1205/cherd.05193.

Almansoori, A., & Shah, N. (2009). Design and operation of a future hydrogen supply chain: Multi-period model. *Int. J. Hydrogen Energy*, *34*, 7883–7897. doi:10.1016/j.ijhydene.2009.07.109.

Berman, O., Bertsimas, D., & Larson, R. C. (1995). Locating discretionary service facilities II: maximizing market size, minimizing inconvenience. *Oper. Res.*, *43*, 623–632. doi:10.1287/opre.43.4.623.

Berman, O., Larson, R. C., & Fouska, N. (1992). Optimal Location of Discretionary Service Facilities. *Transp. Sci.*, *26*, 201–211. doi:10.1287/trsc.26.3.201.

California Air Resources Board (2018). *2018 Annual Evaluation of Fuel Cell Electric Vehicle Deployment and Hydrogen Fuel Station Network Development*. Technical Report California Environmental Protection Agency. URL: https://www.arb.ca.gov/msprog/zevprog/ab8/ab8_report_2018_print.pdf.

Carbon Tracker (2018). EU carbon prices could double by 2021 and quadruple by 2030. URL: https://www.carbontracker.org/eu-carbon-prices-could-double-by-2021-and-quadruple-by-2030/.

Carsalesbase (2018). Automotive Industry analysis, opinions and data. URL: http://carsalesbase.com/.

Chestney, N. (2018). European Union carbon prices climb to 10-year high. URL: https://www.reuters.com/article/eu-carbon-price/update-2-european-union-carbon-prices-climb-to-10-year-high-idUSL5N1V61JD.

Cho, S., bin Woo, Y., Kim, B. S., & Kim, J. (2016). Optimization-based planning of a biomass to

hydrogen (B2H2) system using dedicated energy crops and waste biomass. *Biomass and Bioenergy*, *87*, 144–155. doi:10.1016/j.biombioe.2016.02.025.

Copado-Méndez, P. J., Blum, C., Guillén-Gosálbez, G., & Jiménez, L. (2013). Large neighbourhood search applied to the efficient solution of spatially explicit strategic supply chain management problems. *Comput. Chem. Eng.*, *49*, 114–126. doi:10.1016/j.compchemeng.2012.09.006.

De-León Almaraz, S., Azzaro-Pantel, C., Montastruc, L., & Boix, M. (2015). Deployment of a hydrogen supply chain by multi-objective/multi-period optimisation at regional and national scales. *Chem. Eng. Res. Des.*, *104*, 11–31. doi:10.1016/j.cherd.2015.07.005.

Department of Energy (2010). H2A: Delivery Components Model version 2.0. URL: https://escholarship.org/uc/item/5s85d149.

Department of Energy (2018a). Alternative Fuels Data Center. URL: https://www.afdc.energy.gov/.

Department of Energy (2018b). H2A: Hydrogen Analysis Production Case Studies - Future Central Hydrogen Production via Biomass Gasification version 3.2018. URL: https://www.nrel.gov/hydrogen/h2a-production-case-studies.html.

Department of Energy (2018c). H2A: Hydrogen Analysis Production Case Studies - Future Distributed Hydrogen Production from Natural Gas (1,500 kg per day) version 3.2018. URL: https://www.nrel.gov/hydrogen/h2a-production-case-studies.html.

Department of Energy (2018d). H2A: Hydrogen Analysis Production Case Studies - Future Distributed Hydrogen Production from PEM Electrolysis version 3.2018. URL: https://www.nrel.gov/hydrogen/h2a-production-case-studies.html.

Électricité de France (2018). Emissions de gaz à effet de serre : le relevé mensuel d'EDF. URL: https://www.edf.fr/groupe-edf/nos-engagements/rapports-et-indicateurs/emissions-de-gaz-a-effet-de-serre#bilans-annuels.

Environmental Protection Agency (2018). *Fast Facts: U.S. Transportation Sector GHG Emissions (1990-2016)*. Technical Report. URL: https://nepis.epa.gov/Exe/ZyPDF.cgi?Dockey=P100USI5.pdf.

Eskandarpour, M., Dejax, P., Miemczyk, J., & Péton, O. (2015). Sustainable supply chain network design: An optimization-oriented review. *Omega*, *54*, 11–32. doi:10.1016/j.omega.2015.01.006.

European Environment Agency (2017). *Greenhouse gas emissions from transport*. Technical Report. URL: https://www.eea.europa.eu/data-and-maps/indicators/transport-emissions-of-greenhouse-gases/transport-emissions-of-greenhouse-gases-11.

GlobalPetrolPrices (2019). France diesel prices, 15-Apr-2019 — GlobalPetrolPrices.com. URL: https://www.globalpetrolprices.com/France/diesel{_}prices/.

GRTgaz (2017). *GRTgaz et les territoires*. Technical Report. URL: http://www.grtgaz.com/

fileadmin/plaquettes/fr/2017/GRTgaz-et-les-territoires-12-fiches.pdf.
GRTgaz (2019). Un réseau de transport au cœur des flux gaziers européens. URL: http://www.grtgaz.com/notre-entreprise/notre-reseau.html.
Guillén-Gosálbez, G., Mele, F. D., & Grossmann, I. E. (2010). A bi-criterion optimization approach for the design and planning of hydrogen supply chains for vehicle use. *AIChE J.*, *56*, 650–667. doi:10.1002/aic.12024.
Haynes, K. E., & Fotheringham, A. S. (1985). *Gravity and Spatial Interaction Models*.
He, C., Sun, H., Xu, Y., & Lv, S. (2017). Hydrogen refueling station siting of expressway based on the optimization of hydrogen life cycle cost. *Int. J. Hydrogen Energy*, *42*, 16313–16324. doi:10.1016/j.ijhydene.2017.05.073.
Hodgson, M. J. (1990). A Flow-Capturing Location-Allocation Model. *Geogr. Anal.*, *22*, 270–279. doi:10.1111/j.1538-4632.1990.tb00210.x.
Hosseini, M., & MirHassani, S. A. (2015). Refueling-station location problem under uncertainty. *Transp. Res. Part E Logist. Transp. Rev.*, *84*, 101–116. doi:10.1016/j.tre.2015.10.009.
Hosseini, M., & MirHassani, S. A. (2017). A heuristic algorithm for optimal location of flow-refueling capacitated stations. *Int. Trans. Oper. Res.*, *24*, 1377–1403. doi:10.1111/itor.12209.
Hosseini, M., MirHassani, S. A., & Hooshmand, F. (2017). Deviation-flow refueling location problem with capacitated facilities: Model and algorithm. *Transp. Res. Part D Transp. Environ.*, *54*, 269–281. doi:10.1016/j.trd.2017.05.015.
Huang, Y., Li, S., & Qian, Z. S. (2015). Optimal Deployment of Alternative Fueling Stations on Transportation Networks Considering Deviation Paths. *Networks Spat. Econ.*, *15*, 183–204. doi:10.1007/s11067-014-9275-1.
Hwang, S. W., Kweon, S. J., & Ventura, J. A. (2015). Infrastructure development for alternative fuel vehicles on a highway road system. *Transp. Res. Part E Logist. Transp. Rev.*, *77*, 170–183. doi:10.1016/j.tre.2015.02.011.
Hwangbo, S., Lee, I. B., & Han, J. (2017). Mathematical model to optimize design of integrated utility supply network and future global hydrogen supply network under demand uncertainty. *Appl. Energy*, *195*, 257–267. doi:10.1016/j.apenergy.2017.03.041.
International Energy Agency (2015). *Technology roadmap-hydrogen and fuel cells*. Technical Report. URL: https://www.iea.org/publications/freepublications/publication/TechnologyRoadmapHydrogenandFuelCells.pdf.
International Energy Agency (2017). *Global EV Outlook 2017: Two million and counting*. Technical Report. URL: https://www.iea.org/publications/freepublications/publication/GlobalEVOutlook2017.pdf.
Johnson, N., & Ogden, J. (2012). A spatially-explicit optimization model for long-term hydrogen pipeline planning. *Int. J. Hydrogen Energy*, *37*, 5421–5433. doi:10.1016/j.ijhydene.2011.08.109.

Jung, J., Chow, J. Y., Jayakrishnan, R., & Park, J. Y. (2014). Stochastic dynamic itinerary interception refueling location problem with queue delay for electric taxi charging stations. *Transp. Res. Part C Emerg. Technol.*, *40*, 123–142. doi:10.1016/j.trc.2014.01.008.

Kim, J., Lee, Y., & Moon, I. (2008). Optimization of a hydrogen supply chain under demand uncertainty. *Int. J. Hydrogen Energy*, *33*, 4715–4729. doi:10.1016/j.ijhydene.2008.06.007.

Kim, J., & Moon, I. (2008). Strategic design of hydrogen infrastructure considering cost and safety using multiobjective optimization. *Int. J. Hydrogen Energy*, *33*, 5887–5896. doi:10.1016/j.ijhydene.2008.07.028.

Kim, J. G., & Kuby, M. (2012). The deviation-flow refueling location model for optimizing a network of refueling stations. *Int. J. Hydrogen Energy*, *37*, 5406–5420. doi:10.1016/j.ijhydene.2011.08.108.

Kim, J. G., & Kuby, M. (2013). A network transformation heuristic approach for the deviation flow refueling location model. *Comput. Oper. Res.*, *40*, 1122–1131. doi:10.1016/j.cor.2012.10.021.

Kuby, M., & Lim, S. (2005). The flow-refueling location problem for alternative-fuel vehicles. *Socioecon. Plann. Sci.*, *39*, 125–145. doi:10.1016/j.seps.2004.03.001.

Kuby, M., Lines, L., Schultz, R., Xie, Z., Kim, J. G., & Lim, S. (2009). Optimization of hydrogen stations in Florida using the Flow-Refueling Location Model. *Int. J. Hydrogen Energy*, *34*, 6045–6064. doi:10.1016/j.ijhydene.2009.05.050.

L'Association Française pour l'Hydrogène et les Piles à Combustible (2018). Mobilité hydrogène France. URL: http://www.afhypac.org/mobilite-hydrogene-france/.

Li, L., Manier, H., & Manier, M.-A. (2019). Hydrogen supply chain network design : An optimization-oriented review. *Renew. Sustain. Energy Rev.*, *103*, 342–360. doi:10.1016/j.rser.2018.12.060.

Lim, S., & Kuby, M. (2010). Heuristic algorithms for siting alternative-fuel stations using the Flow-Refueling Location Model. *Eur. J. Oper. Res.*, *204*, 51–61. doi:10.1016/j.ejor.2009.09.032.

Lin, Z., Ogden, J., Fan, Y., & Chen, C. W. (2008). The fuel-travel-back approach to hydrogen station siting. *Int. J. Hydrogen Energy*, *33*, 3096–3101. doi:10.1016/j.ijhydene.2008.01.040.

L'Institut national de la statistique et des études économiques (2015a). Fichier Mobilités professionnelles des individus - Logements, individus, activité, mobilités scolaires et professionnelles en 2012. URL: https://insee.fr/fr/statistiques/1913213?sommaire=1912584&q=Mobilit%27es+professionnelles+2012.

L'Institut national de la statistique et des études économiques (2015b). Populations légales 2013. URL: https://www.insee.fr/fr/statistiques/2387611?sommaire=2119504.

L'Institut national de la statistique et des études économiques (2018a). Comparateur de territoire. URL: https:

//insee.fr/fr/statistiques/zones/1405599?debut=0&q=Comparateur+de+territoire.
L'Institut national de la statistique et des études économiques (2018b). Statistiques locales - Indicateurs : cartes, données et graphiques. URL: https://statistiques-locales.insee.fr/#view=map1&c=indicator.
M. Ruth, T.A. Timbario, T. T., & Laffen, M. (2011). *Methodology for Calculating Cost per Mile for Current and Future Vehicle Powertrain Technologies , with Projections to 2024*. Technical Report National Renewable Energy Laboratory. URL: https://www.nrel.gov/docs/fy11osti/49231.pdf. doi:10.4271/2011-01-1345.
McKinsey & Company (2017). *Hydrogen scaling up: A sustainable pathway for the global energy transition*. Technical Report Hydrogen Council. URL: http://hydrogencouncil.com/wp-content/uploads/2017/11/Hydrogen-scaling-up-Hydrogen-Council.pdf.
Melaina, M., & Penev, M. (2013). *Hydrogen Station Cost Estimates: Comparing Hydrogen Station Cost Calculator Results with other Recent Estimates*. Technical Report National Renewable Energy Laboratory. URL: https://www.nrel.gov/docs/fy13osti/56412.pdf.
Melendez, M., & Milbrandt, A. (2006). *Geographically Based Hydrogen Consumer Demand and Infrastructure Analysis*. Technical Report National Renewable Energy Laboratory. URL: https://www.nrel.gov/docs/fy07osti/40373.pdf.
Melendez, M., & Milbrandt, A. (2008). *Regional Consumer Hydrogen Demand and Optimal Hydrogen Refueling Station Siting*. Technical Report National Renewable Energy Laboratory. URL: https://www.nrel.gov/docs/fy08osti/42224.pdf.
Melo, M., Nickel, S., & Saldanha-da Gama, F. (2009). Facility location and supply chain management – A review. *European Journal of Operational Research*, *196*, 401–412. URL: https://www.sciencedirect.com/science/article/pii/S0377221708004104?via%3Dihub. doi:10.1016/J.EJOR.2008.05.007.
Ministère de la Transition écologique et solidaire (2018). *National low carbon strategy project*. Technical Report. URL: https://www.ecologique-solidaire.gouv.fr/sites/default/files/Projet%20SNBC%20EN.pdf.
Moreno-Benito, M., Agnolucci, P., & Papageorgiou, L. G. (2017). Towards a sustainable hydrogen economy: Optimisation-based framework for hydrogen infrastructure development. *Comput. Chem. Eng.*, *102*, 110–127. doi:10.1016/j.compchemeng.2016.08.005.
Mula, J., Peidro, D., Díaz-Madroñero, M., & Vicens, E. (2010). Mathematical programming models for supply chain production and transport planning. *Eur. J. Oper. Res.*, *204*, 377–390. doi:10.1016/j.ejor.2009.09.008.
Murthy Konda, N. V. S. N., Shah, N., & Brandon, N. P. (2011). Optimal transition towards a large-scale hydrogen infrastructure for the transport sector: The case for the Netherlands. *Int. J. Hydrogen Energy*, *36*, 4619–4635. doi:10.1016/j.ijhydene.2011.01.104.
National Renewable Energy Laboratory (2011). *Hydrogen Production Cost Estimate Using Biomass Gasification Independent Review*. Technical Report. URL:

https://www.energy.gov/sites/prod/files/2014/03/f9/51726.pdf.
Nicholas, M., Handy, S., & Sperling, D. (2004). Using Geographic Information Systems to Evaluate Siting and Networks of Hydrogen Stations. *Transp. Res. Rec. J. Transp. Res. Board*, *1880*, 126–134. doi:10.3141/1880-15.
Nicholas, M., & Ogden, J. (2006). Detailed Analysis of Urban Station Siting for California Hydrogen Highway Network. *Transp. Res. Rec. J. Transp. Res. Board*, *1983*, 121–128. doi:10.3141/1983-17.
Ogumerem, G. S., Kim, C., Kesisoglou, I., Diangelakis, N. A., & Pistikopoulos, E. N. (2018). A multi-objective optimization for the design and operation of a hydrogen network for transportation fuel. *Chem. Eng. Res. Des.*, . doi:10.1016/j.cherd.2017.12.032.
Parker, N., Fan, Y., & Ogden, J. (2010). From waste to hydrogen: An optimal design of energy production and distribution network. *Transp. Res. Part E Logist. Transp. Rev.*, *46*, 534–545. doi:10.1016/j.tre.2009.04.002.
RentalYard (2018). Chemical / Acid Tank Trailers For Rent. URL: https://www.rentalyard.com/listings/trailers/for-rent/list/category/69/tank-trailers-chemical-acid.
Samsatli, S., & Samsatli, N. J. (2015). A general spatio-temporal model of energy systems with a detailed account of transport and storage. *Comput. Chem. Eng.*, *80*, 155–176. doi:10.1016/j.compchemeng.2015.05.019.
Shukla, A., Pekny, J., & Venkatasubramanian, V. (2011). An optimization framework for cost effective design of refueling station infrastructure for alternative fuel vehicles. *Comput. Chem. Eng.*, *35*, 1431–1438. doi:10.1016/j.compchemeng.2011.03.018.
Sims, R., Schaeffer, R., Creutzig, F., Cruz-Núñez, X., & D'Agosto, M. (2014). *Transport. In: Climate Change 2014: Mitigation of Climate Change. Contribution of Working Group III to the Fifth Assessment Report of the Intergovernmental Panel on Climate Change*. Technical Report. URL: https://www.ipcc.ch/site/assets/uploads/2018/02/ipcc_wg3_ar5_chapter8.pdf.
Statista (2019a). Industry prices for electricity in France 2008-2017. URL: https://www.statista.com/statistics/595816/electricity-industry-price-france/.
Statista (2019b). Industry prices of natural gas in France 2008-2017. URL: https://www.statista.com/statistics/595626/natural-gas-price-france/.
Sun, H., He, C., Wang, H., Zhang, Y., Lv, S., & Xu, Y. (2017). Hydrogen station siting optimization based on multi-source hydrogen supply and life cycle cost. *Int. J. Hydrogen Energy*, *42*, 23952–23965. doi:10.1016/j.ijhydene.2017.07.191.
Upchurch, C., Kuby, M., & Lim, S. (2009). A model for location of capacitated alternative-fuel stations. *Geogr. Anal.*, *41*, 127–148. doi:10.1111/j.1538-4632.2009.00744.x.
Van Den Heever, S. A., & Grossmann, I. E. (2003). A strategy for the integration of production planning and reactive scheduling in the optimization of a hydrogen supply network. *Comput. Chem. Eng.*, *27*, 1813–1839. doi:10.1016/S0098-1354(03)00158-3.
Wang, Y.-W., & Lin, C.-C. (2009). Locating road-vehicle refueling stations. *Transp. Res. Part E*

Logist. Transp. Rev., *45*, 821–829. doi:10.1016/J.TRE.2009.03.002.

Wang, Y. W., & Lin, C. C. (2013). Locating multiple types of recharging stations for battery-powered electric vehicle transport. *Transp. Res. Part E Logist. Transp. Rev.*, *58*, 76–87. doi:10.1016/j.tre.2013.07.003.

Wang, Y. W., & Wang, C. R. (2010). Locating passenger vehicle refueling stations. *Transp. Res. Part E Logist. Transp. Rev.*, *46*, 791–801. doi:10.1016/j.tre.2009.12.001.

Won, W., Kwon, H., Han, J. H., & Kim, J. (2017). Design and operation of renewable energy sources based hydrogen supply system: Technology integration and optimization. *Renew. Energy*, *103*, 226–238. doi:10.1016/j.renene.2016.11.038.

Woo, Y. B., Cho, S., Kim, J., & Kim, B. S. (2016). Optimization-based approach for strategic design and operation of a biomass-to-hydrogen supply chain. *Int. J. Hydrogen Energy*, *41*, 5405–5418. doi:10.1016/j.ijhydene.2016.01.153.

World Bank, & Ecofys (2018). *State and Trends of Carbon Pricing 2018*. Technical Report. URL: https://openknowledge.worldbank.org/bitstream/handle/10986/29687/9781464812927.pdf?sequence=5&isAllowed=y.

Appendices

A. Nomenclature

Parameters

α	annual network operating period, d/y
β	payback period of capital investment, y
γ^{e}_{sij}	standard fueling station emission factor, kg CO_2/kg H_2
γ^{e}_{oj}	on-site fueling station emission factor, kg CO_2/kg H_2
γ^{e}_{h}	emission factor of hydrogen transportation mode h, kg CO_2/L fuel
γ^{c}_{pik}	production emission capture efficiency
γ^{eo}_{pik}	production on-site emission factor, kg CO_2/kg H_2
γ^{eu}_{pik}	production upstream emission factor, kg CO_2/kg H_2
$\delta_{(e,o)}$	conversion rates of feedstock to hydrogen (for on-site fueling stations), unit feedstock/kg H_2
$\delta_{(e,p)}$	conversion rates of feedstock to hydrogen (for hydrogen production plants), unit feedstock/kg H_2
ϵ	a small positive number
$ccap^{max}_{n}$	upper limit of CO_2 processing capacity, kg CO_2/d
$ccap^{min}_{n}$	lower limit of CO_2 processing capacity, kg CO_2/d

ccc	capital cost of a CO_2 storage site, €
coc	operating cost of CO_2 processing, €/kg CO_2
cp	carbon price, €/kg CO_2
$cpcc$	capital cost of CO_2 pipeline, €/km
$dem^{h,exp}$	percentage of hydrogen demand flow that expected to be captured, %
$dem_{ni}^{h,A}$	fixed-location hydrogen demand (Type A) of each node, kg H_2/d
$dem_{ni}^{h,B}$	fixed-location hydrogen demand (Type B) of each node, kg H_2/d
dw_h	driver wage of hydrogen transportation mode h, €/h
dw_f	driver wage of feedstock transportation mode f, €/h
$ecap_{ne}^{max}$	upper limit of feedstock supply capacity at each node, unit feedstock/d
$ecap_{ne}^{min}$	lower limit of feedstock supply capacity at each node, unit feedstock/d
eoc_e	operating cost of a feedstock site, €/d
euc_e	feedstock unit cost, €/unit feedstock
$fcap_{sij}^{max}$	upper limit of standard fueling capacity, kg H_2/d
$fcap_{sij}^{min}$	lower limit of standard fueling capacity, kg H_2/d
$fcap_{oj}^{max}$	upper limit of on-site fueling capacity, kg H_2/d
$fcap_{oj}^{min}$	lower limit of on-site fueling capacity, kg H_2/d
fcc_{sij}	capital cost of a standard fueling station, €
fcc_{oj}	capital cost of an on-site fueling station, €
fe_h	fuel economy of hydrogen transportation mode h, km/L fuel
fe_f	fuel economy of feedstock transportation mode f, km/L fuel
f_n^{node}	hydrogen fueling demand flow of each node, kg H_2/d
foc_{sij}	operating cost of a standard fueling station, €/kg H_2
foc_{oj}	operating cost of an on-site fueling station, €/kg H_2
fp_h	fuel price of hydrogen transportation mode h, €/L fuel
fp_f	fuel price of feedstock transportation mode f, €/L fuel
f_q^{pair}	hydrogen fueling demand flow of each OD (Origin–Destination) pair, kg H_2/d
ge_h	general expense of hydrogen transportation mode h, €/d
ge_f	general expense of feedstock transportation mode f, €/d
$id_n^{h,A}$	equals 1 if there exists fixed-location hydrogen demand (Type A) at this node (0 otherwise)
$id_n^{h,B}$	equals 1 if there exists fixed-location hydrogen demand (Type B) at this node (0 otherwise)
l_{nm}	the shortest distance between two different nodes, km
lut_h	load/unload time of hydrogen transportation mode h, h
lut_f	load/unload time of feedstock transportation mode f, h
me_h	maintenance expense of hydrogen transportation mode h, €/km
me_f	maintenance expense of feedstock transportation mode f, €/km

$pcap_{pik}^{max}$	upper limit of production capacity, kg H_2/d
$pcap_{pik}^{min}$	lower limit of production capacity, kg H_2/d
pcc_{pik}	capital cost of a production plant, €
poc_{pik}	operating cost of a production plant, €/kg H_2
sp_h	speed of hydrogen transportation mode h, km/h
sp_f	speed of feedstock transportation mode f, km/h
$tcap_h$	capacity of hydrogen transportation mode h, kg H_2
$tcap_f$	capacity of feedstock transportation mode f, unit feedstock
$tcap_h^{max}$	upper limit of hydrogen transportation capacity between two nodes, kg H_2/d
$tcap_f^{max}$	upper limit of feedstock transportation capacity between two nodes, unit feedstock/d
$tcap_h^{min}$	lower limit of hydrogen transportation capacity between two nodes, kg H_2/d
$tcap_f^{min}$	lower limit of feedstock transportation capacity between two nodes, unit feedstock/d
$tcap^{max}$	upper limit of CO_2 transportation capacity, kg CO_2/d
$tcap^{min}$	lower limit of CO_2 transportation capacity, kg CO_2/d
tcr_h	vehicle rental cost of hydrogen transportation mode h (for each vehicle), €/d
tcr_f	vehicle rental cost of feedstock transportation mode f (for each vehicle), €/d
tma_h	availability of hydrogen transportation mode h, h/d
tma_f	availability of feedstock transportation mode f, h/d

Continuous variables

CC	total daily capital cost, €/d
CR	total processing rate of CO_2, kg CO_2/d
CR_n	CO_2 processing rate of a CO_2 storage site, kg CO_2/d
$DEM^{h,cap}$	percentage of hydrogen demand flow that could be captured, %
EC	daily feedstock purchasing cost, €/d
EMC	daily emission cost, €/d
ER	total emission rate, kg CO_2/d
ESR_e	total feedstock supply rate of feedstock sites, unit feedstock/d (feedstock type e)
FCC	daily facility capital cost, €/d
FFC	daily feedstock transportation fuel cost, €/d
FGC	daily feedstock transportation general cost, €/d
FLC	daily feedstock transportation labor cost, €/d
FMC	daily feedstock transportation maintenance cost, €/d
FOC	daily facility operating cost, €/d
FR_{noj}	fueling rate of an on-site fueling station, kg H_2/d

	(fueling technology o, size j)
FR_{nsij}	fueling rate of a standard fueling station, kg H_2/d
	(fueling technology s, hydrogen form i, size j)
FR_{oj}	total fueling rate of on-site fueling stations, kg H_2/d
	(fueling technology o, size j)
FR_{sij}	total fueling rate of standard fueling stations, kg H_2/d
	(fueling technology s, hydrogen form i, size j)
FRC	daily feedstock transportation vehicle rental cost, €/d
$FTOC$	daily feedstock transportation operating cost, €/d
HFC	daily hydrogen transportation fuel cost, €/d
HGC	daily hydrogen transportation general cost, €/d
HLC	daily hydrogen transportation labor cost, €/d
HMC	daily hydrogen transportation maintenance cost, €/d
HRC	daily hydrogen transportation vehicle rental cost, €/d
$HTOC$	daily hydrogen transportation operating cost, €/d
$LCOH$	least cost of hydrogen, €/kg H_2
OC	total daily operating cost, €/d
$OESR_{ne}$	feedstock supply rate for the on-site fueling station at node n, unit feedstock/d
	(feedstock type e)
$OFER$	total emission rate of on-site fueling stations, kg CO_2/d
PER	total production emission rate, kg CO_2/d
PER^c	total emission rate of production plants where emissions are processed, kg CO_2/d
PER^c_n	emission rate of a production plant where emissions are processed, kg CO_2/d
$PESR_{ne}$	feedstock supply rate for production plants at node n or built at other nodes,
	unit feedstock/d, (feedstock type e)
PR^c_{npik}	production rate of a production plant where emissions are processed, kg H_2/d
PR_{npik}	production rate of a production plant, kg H_2/d
	(production technology p, hydrogen form i, size k)
PR_{pik}	total production rate of production plants, kg H_2/d
	(production technology p, hydrogen form i, size k)
Q_{fnm}	feedstock transportation flux from node n to m, unit feedstock/d
	(transportation mode f)
Q_{hnm}	hydrogen transportation flux from node n to m, kg H_2/d (transportation mode h)
Q_{nm}	CO_2 transportation flux from node n to m, kg CO_2/d
$SFER$	total emission rate of standard fueling stations, kg CO_2/d
TCC	daily CO_2 transportation capital cost, €/d
TDC	total daily cost, €/d
TER	total emission rate of hydrogen transportation, kg CO_2/d

THD	the amount of hydrogen delivered per day, kg H_2/d

Integer variables

NE_e	number of feedstock supply sites (for hydrogen production plants) (feedstock type e)
NF_{sij}	number of standard fueling stations (fueling technology s, hydrogen form i, size j)
NF_{oj}	number of on-site fueling stations (fueling technology o, size j)
NP_{pik}	number of production plants (production technology p, hydrogen form i, size k)
NR	number of CO_2 storage reservoirs
NV_h	number of hydrogen transportation vehicles
NV_f	number of feedstock transportation vehicles

Binary variables

IC_q	1 if hydrogen fueling demand flow pair q is captured
IE_n	1 if the node is chosen as a feedstock supplier of production plants
IE_{ne}	1 if the node is chosen as a feedstock supplier of production plants (feedstock type e)
IF_n	1 if there is a fueling station at this node
IF_{no}	1 if there is an on-site fueling station at this node (fueling technology o)
IF_{nsij}	1 if there is a standard fueling station at this node (fueling technology s, hydrogen form i, size j)
IF_{noj}	1 if there is an on-site fueling station at this node (fueling technology o, size j)
IM_n	1 if the emission of production plant at this node is processed
IP_n	1 if there is a production plant at this node
IP_{npik}	1 if there is a production plant at this node (production technology p, hydrogen form i, size k)
IR_n	1 if there is a CO_2 storage site at this node
OIF_n	1 if there is an on-site fueling station at this node
SIF_n	1 if there is a standard fueling station at this node
X_{fnm}	1 if feedstock is to be transported from node n to m in transportation mode f
X_{hnm}	1 if hydrogen is to be transported from node n to m in transportation mode h
X_{nm}	1 if CO_2 is to be transported from node n to m

B. Case study inputs

Table B.1: Population and demographic metrics values of 31 cities

City	Population (person)	Vehicle (%)	Income (€/year)	Education (%)	Commute (%)
Baume-les-Dames	5,255	55.45	19,395	12.90	73.87
Bavans	3,701	68.25	20,224	15.70	81.31
Beaucourt	5,047	63.96	19,884	14.70	82.29
Belfort	63,683	37.22	17,604	15.03	63.88
Besançon	116,690	33.11	18,583	15.80	61.65
Champagnole	7,908	45.91	19,059	14.10	72.08
Delle	5,773	54.42	19,483	15.20	76.37
Dole	23,312	46.34	18,813	15.40	71.09
Fougerolles	5,504	36.90	15,679	15.80	67.62
Gray	3,721	71.08	19,023	15.00	83.78
Hauts de Bienne	5,457	48.44	19,561	12.80	72.18
Héricourt	9,967	60.50	18,630	14.00	79.25
Hérimoncourt	3,635	60.87	19,600	15.50	84.24
Lons-le-Saunier	17,311	34.21	18,185	17.90	63.87
Lure	8,324	46.88	17,174	14.80	68.98
Luxeuil-les-Bains	6,917	46.83	17,003	14.80	73.67
Maîche	4,233	59.06	23,853	15.00	85.30
Montbéliard	40,733	46.28	16,734	13.37	73.98
Morteau	6,827	51.62	27,219	18.50	77.14
Ornans	4,329	57.94	20,775	15.50	71.81
Poligny	4,146	51.53	18,975	17.00	68.40
Pontarlier	17,413	45.44	21,995	16.70	71.36
Pont-de-Roide-Vermondans	4,230	62.47	19,497	14.70	75.54
Saint-Claude	10,096	45.11	18,032	12.40	68.70
Saint-Loup-sur-Semouse	3,263	52.00	15,493	12.00	68.40
Saint-Vit	4,803	60.38	20,718	16.40	83.40
Tavaux	3,957	63.91	21,373	15.80	82.25
Valdahon	5,344	44.76	20,614	20.20	63.22
Valentigney	34,877	57.10	17,875	13.86	79.72
Vesoul	15,212	34.31	17,159	14.50	66.37
Villers-le-Lac	4,750	65.32	30,370	16.60	88.26

Source: Population, Income - (L'Institut national de la statistique et des études économiques, 2018a); Vehicle, Commute - (L'Institut national de la statistique et des études économiques, 2015a); Education - (L'Institut national de la statistique et des études économiques, 2018b).
Note: Combinations of adjacent cities -
Belfort = Belfort+Bavilliers+Offemont+Valdoie;
Montbéliard = Montbéliard+Bethoncourt+Grand Charmont+Sochaux;
Valentigney = Valentigney+Audincourt+Seloncourt+Mandeure;
The values of combined cities are obtained by weighted average method (on population).

Table B.2: Production technology - steam methane reforming (SMR)

	Hydrogen form:	Gaseous			Liquid			Source
	Facility size:	Small	Medium	Large	Small	Medium	Large	
Capital cost	million €	1.05	1.70	2.28	10.62	16.70	21.78	(1)
Operating cost	€/kg H_2	0.34	0.31	0.30	2.65	2.15	1.93	(2)
Maximum capacity	1,000 kg/d	2.00	3.50	5.00	2.00	3.50	5.00	
Minimum capacity	1,000 kg/d	1.00	2.50	4.00	1.00	2.50	4.00	
Upstream emission factor	kg CO_2/kg H_2	2.40	2.40	2.40	3.07	3.00	2.97	(3)
On-site emission factor	kg CO_2/kg H_2	8.66	8.66	8.66	8.66	8.66	8.66	(4)
Emission capture efficiency		0.90	0.90	0.90	0.90	0.90	0.90	(5)

Source: (1), (2), (4) - (Department of Energy, 2010, 2018c); (3) - (Department of Energy, 2010, 2018c; Électricité de France, 2018); (5) - (Department of Energy, 2018b).
Note: The costs of liquid production (capital and operating) are obtained by adding the cost of liquefier to gaseous production.

Table B.3: Production technology - Electrolysis

	Hydrogen form:	Gaseous			Liquid			Source
	Facility size:	Small	Medium	Large	Small	Medium	Large	
Capital cost	million €	1.74	2.62	3.92	11.32	17.62	23.43	(1)
Operating cost	€/kg H_2	0.17	0.14	0.11	2.48	1.98	1.74	(2)
Maximum capacity	1,000 kg/d	2.00	3.50	5.00	2.00	3.50	5.00	
Minimum capacity	1,000 kg/d	1.00	2.50	4.00	1.00	2.50	4.00	
Upstream emission factor	kg CO_2/kg H_2	1.96	1.57	1.26	2.63	2.17	1.83	(3)
On-site emission factor	kg CO_2/kg H_2	-	-	-	-	-	-	
Emission capture efficiency		0.90	0.90	0.90	0.90	0.90	0.90	(4)

Source: (1), (2) - (Department of Energy, 2010, 2018d); (3) - (Department of Energy, 2010, 2018d; Électricité de France, 2018); (4) - (Department of Energy, 2018b).
Note: The costs of liquid production (capital and operating) are obtained by adding the cost of liquefier to gaseous production;
Because lack of information, the upstream emission factor of "Medium" and "Large" (gaseous production) are obtained by multiplying the value of "Small" with 0.8 and 0.64, respectively.

Table B.4: Production technology - biomass gasification (BG)

	Hydrogen form:	Gaseous			Liquid			Source
	Facility size:	Small	Medium	Large	Small	Medium	Large	
Capital cost	million €	4.09	7.03	9.64	13.67	22.03	29.15	(1)
Operating cost	€/kg H_2	4.01	2.48	1.90	6.32	4.33	3.52	(2)
Maximum capacity	1,000 kg/d	2.00	3.50	5.00	2.00	3.50	5.00	
Minimum capacity	1,000 kg/d	1.00	2.50	4.00	1.00	2.50	4.00	
Upstream emission factor	kg CO_2/kg H_2	-22.26	-22.26	-22.26	-21.59	-21.66	-21.69	(3)
On-site emission factor	kg CO_2/kg H_2	24.00	24.00	24.00	24.00	24.00	24.00	(4)
Emission capture efficiency		0.90	0.90	0.90	0.90	0.90	0.90	(5)

Source: (1), (2), (4) - (Department of Energy, 2010, 2018b); (3) - (Department of Energy, 2010, 2018b; Électricité de France, 2018); (5) - (Department of Energy, 2018b).
Note: The costs of a liquid production plant (capital and operating) are obtained by adding the cost of a liquefier to a gaseous production plant.
The upstream emission factors are negative because the plants that are the source of biomass capture a certain amount of CO_2 through photosynthesis while they are growing.

Table B.5: Standard fueling technology

	Hydrogen form:	Gaseous				Liquid				Source
	Facility size:	Small	Medium	Large	Extra-large	Small	Medium	Large	Extra-large	
Capital cost	million €	1.08	1.87	2.10	4.21	1.16	1.52	1.57	3.14	(1)
Operating cost	€/kg H_2	3.28	2.20	1.28	1.28	5.39	2.66	1.45	1.45	(2)
Maximum capacity	1,000 kg/d	0.15	0.30	0.60	1.20	0.15	0.30	0.60	1.20	(3)
Minimum capacity	1,000 kg/d	0.05	0.15	0.30	0.60	0.05	0.15	0.30	0.60	(4)
Emissions factor	kg CO_2/kg H_2	2.34	2.07	1.59	1.59	0.42	0.41	0.41	0.41	(5)

Source: (1), (2), (5) - (Department of Energy, 2010); (3), (4) - (L'Association Française pour l'Hydrogène et les Piles à Combustible, 2018).

Table B.6: On-site fueling technologies

	On-site fueling techn.:	On-site-SMR				On-site-electrolysis				Source
	Facility size:	Small	Medium	Large	Extra-large	Small	Medium	Large	Extra-large	
Capital cost	million €	1.26	2.18	2.59	5.19	1.32	2.27	2.75	5.50	(1)
Operating cost	€/kg H_2	4.57	3.31	2.21	2.21	4.15	2.97	1.79	1.79	(2)
Maximum capacity	1,000 kg/d	0.15	0.30	0.60	1.20	0.15	0.30	0.60	1.20	(3)
Minimum capacity	1,000 kg/d	0.05	0.15	0.30	0.60	0.05	0.15	0.30	0.60	(4)
Emissions factor	kg CO_2/kg H_2	19.49	16.25	13.54	13.54	5.34	4.45	3.71	3.71	(5)

Source: (1), (2) - (Department of Energy, 2018c,d; Melaina & Penev, 2013); (3), (4) - (L'Association Française pour l'Hydrogène et les Piles à Combustible, 2018); (5) - (Department of Energy, 2018c,d; Électricité de France, 2018).
Note: The costs of an on-site station (capital and operating) are obtained by adding the cost of on-site production to a gaseous standard station.
Due to lack of information, the emission factor of "Medium" and "Small" are obtained by multiplying the value of "Large" with 1.2 and 1.44, respectively.

Table B.7: Hydrogen and feedstock transportation: cost and emission data

		Hydrogen		Biomass	Source
		Tube trailer	Tanker truck	Truck	
Driver wage	€/h	20.47	20.47	20.47	(1)
Fuel economy	km/L	2.55	2.55	2.55	(2)
Fuel price	€/L	1.46	1.46	1.46	(3)
General expenses	€/d	7.32	7.32	7.32	(4)
Load/unload time	h	2.00	2.00	2.00	(5)
Maintenance expenses	€/km	0.09	0.09	0.09	(6)
Average speed	km/h	55.00	55.00	55.00	(7)
Availability	h/d	18.00	18.00	18.00	(8)
Emissions factor	kg CO_2/L	2.68	2.68	2.68	(9)
Capacity	1,000 kg	0.18	4.08	8.00	(10)
Vehicle rental cost	€/d	71.20	89.00	44.50	(11)
Maximum transport capacity	1,000 kg/d	5.00	5.00	69.40	
Minimum transport capacity	1,000 kg/d	0.05	0.05	8.00	

Source: (1), (2), (4), (5), (6), (7), (8) - (Almansoori & Shah, 2006); (3) - (GlobalPetrolPrices, 2019); (9) - (Almansoori & Betancourt-Torcat, 2016); (10) - (Almansoori & Shah, 2006; RentalYard, 2018); (11) - (RentalYard, 2018).
Note: The maximum transport capacity is based on the assumption that individual modes cannot transport more than what is produced by a large production facility.

Table B.8: Feedstock prices, conversion rates, and CCS system inputs

Parameter		Value	Source
Natural gas price	€/Nm^3	0.36	(1)
Electricity price	€/kWh	0.10	(2)
Biomass price	€/kg	0.05	(3)
Conversion rate (SMR)	Nm^3 Natural gas/kg H_2	4.61	(4)
Conversion rate (Electrolysis)	kWh Electricity/kg H_2	54.60	(5)
Conversion rate (BG)	kg Biomass/kg H_2	13.88	(6)
CCS capital cost	million €	2.03	(7)
CO_2 pipeline capital cost	million €/km	0.08	(8)
CO_2 processing cost	€/kg	0.09	(9)
CO_2 transport capacity (Max)	1,000 kg/d	500.00	
CO_2 transport capacity (Min)	1,000 kg/d	-	

Source: (1) - (Statista, 2019b); (2) - (Statista, 2019a); (3), (6) - (National Renewable Energy Laboratory, 2011); (4) - (Department of Energy, 2018c); (5) - (Department of Energy, 2018d); (7), (8), (9) - (Department of Energy, 2018b)

C. Supplementary material

Supplementary material can be found in the submission files, with the name of *Supplementary-Material.pdf*.

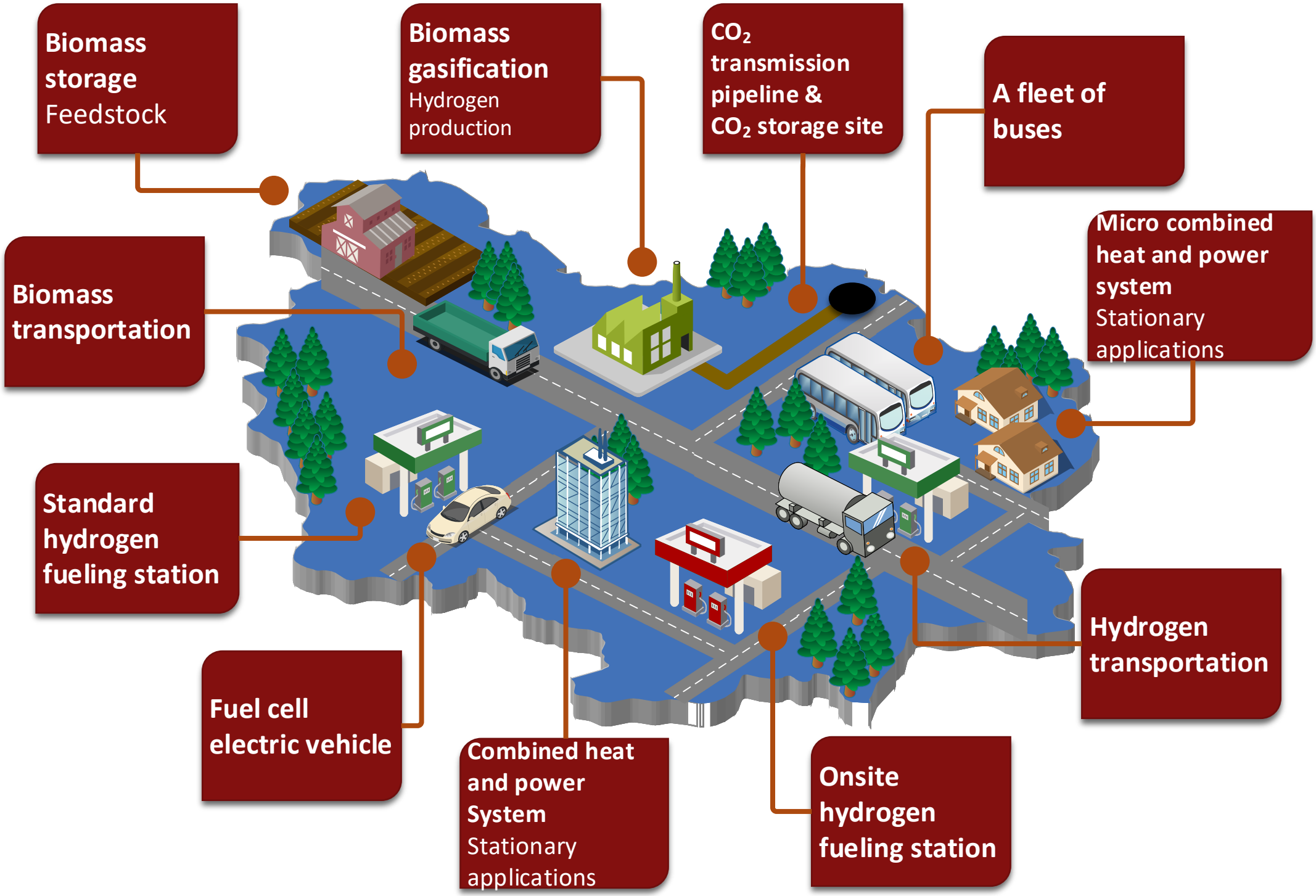
Biomass storage
Feedstock
Biomass gasification
Hydrogen production
CO_2 transmission pipeline & CO_2 storage site
A fleet of buses
Micro combined heat and power system
Stationary applications
Biomass transportation
Standard hydrogen fueling station
Fuel cell electric vehicle
Combined heat and power System
Stationary applications
Onsite hydrogen fueling station
Hydrogen transportation